

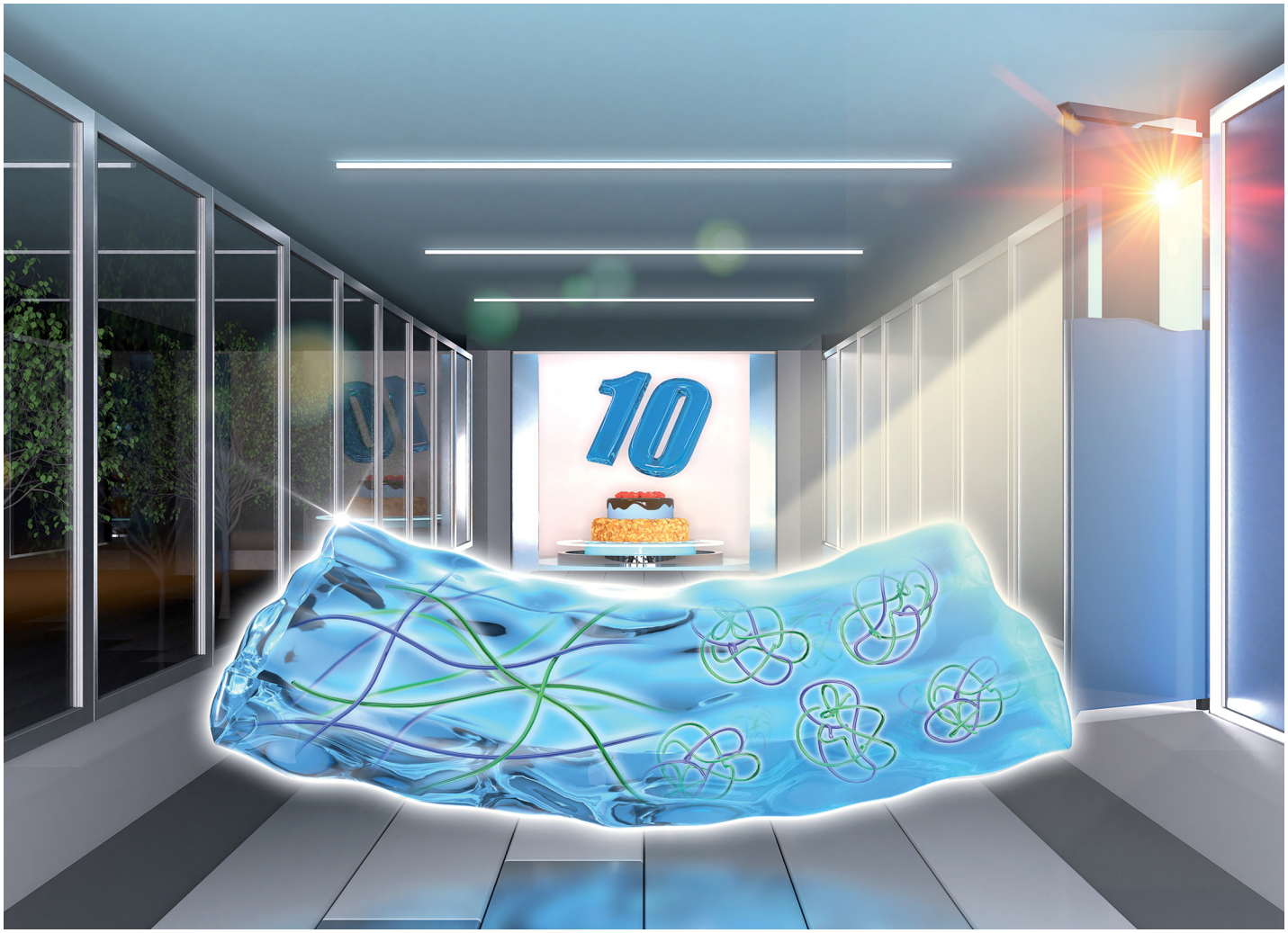
https://dspace.org/

# Thermochromic hydrogelbased energy efficient smart windows fabrication mechanisms and advancements

**Gang Xu; Yucan Lu; Xinguantong Zhou; Nosipho Moloto; E et al**

https://hdl.handle.net/10539/43598
WOS

Downloaded from a DSpace repository. https://dspace.org/




**Showcasing a review by Wei Zhang, ZhengMing Sun and colleagues at School of Materials Science and Engineering, Southeast University, Nanjing, China, School of Chemistry, University of the Witwatersrand, Johannesburg, South Africa, and Nagoya Institute of Technology, Japan.**

Thermochromic hydrogel-based energy efficient smart windows: fabrication, mechanisms, and advancements

This review presents a comprehensive overview of recent advancements in hydrogel-based thermochromic smart windows, focusing on fabrication strategies, chromic mechanisms, and improvements in responsiveness, stability and energy-saving performance.

## As featured in:




See Wei Zhang, ZhengMing Sun *et al.*, *Mater. Horiz.*, 2024, **11**, 4867.

ROYAL SOCIETY OF CHEMISTRY

rsc.li/materials-horizons

Registered charity number: 207890

Materials Horizons

ROYAL SOCIETY OF CHEMISTRY

REVIEW

View Article Online
View Journal | View Issue

Published on 18 September 2024. Downloaded by University of the Witwatersrand on 12/12/2024 3:02:43 PM.

Check for updates

Cite this: *Mater. Horiz.*, 2024, **11**, 4867

# Thermochromic hydrogel-based energy efficient smart windows: fabrication, mechanisms, and advancements

Gang Xu,[a] Yucan Lu,[a] Xinguantong Zhou,[a] Nosipho Moloto,[b] Jiacheng Liu,[c] Song-Zhu Kure-Chu,[c] Takehiko Hihara,[c] Wei Zhang *[a] and ZhengMing Sun *[a]

Received 12th July 2024,
Accepted 13th September 2024

DOI: 10.1039/d4mh00903g

rsc.li/materials-horizons

Thermochromic smart windows are regarded as highly cost-effective and easily implementable strategies with zero energy input among the smart window technologies. They possess the capability to spontaneously adjust between transparent and opaque states according to the ambient temperatures, which is essential for energy-efficient buildings. Recently, thermochromic smart windows based on hydrogels with various chromic mechanisms have emerged to meet the increasing demand for energy-saving smart windows. This review provides an overview of recent advancements in hydrogel-based thermochromic smart windows, focusing on fabrication strategies, chromic mechanisms, and improvements in responsiveness, stability and energy-saving performance. Key developments include dual-responsiveness, tunable critical transition temperatures, freezing resistance, and integrations with radiative cooling/power generation technologies. Finally, we also offer a perspective on the future development of thermochromic smart windows utilizing hydrogels. We hope that this review will enhance the understanding of the chromic mechanism of thermochromic hydrogels, and bring new insights and inspirations on the further design and development of thermochromic hydrogels and derived smart windows.

**Wider impact**

Thermochromic hydrogels, one of the most-studied thermochromic materials, have captured significant attention in the field of energy-saving smart windows due to their exceptional combination of high luminous transmittance ($T_{lum}$), solar energy modulation ($\Delta T_{sol}$), and tunable critical transition temperature ($\tau_c$). Considerable research has been dedicated to designing and synthesizing a variety of thermochromic hydrogels. This review provides a comprehensive overview of the recent progress in hydrogel-based thermochromic smart windows, emphasizing their fabrication, chromic mechanisms, and advancements. The chromic mechanism of thermochromic hydrogels has long been attributed to phase separation between the hydrogel network and water, while the phase separation varies among different types of hydrogels. Thus, it is crucial to understand the chromic mechanism of thermochromic hydrogels from a molecular perspective. Besides, over the past decade, thermochromic hydrogel-based smart windows have witnessed rapid development, with continuously improving thermochromic performance, stability and multifunctionalities. These advancements include higher $T_{lum}$ and $\Delta T_{sol}$, as well as new features like dual-responsiveness, tunable $\tau_c$, freezing resistance, radiative cooling, and power generation. This review will help researchers identify the inherent chromic mechanisms and understand the emerging research trends of thermochromic hydrogels, offering a new insight for the future development of hydrogel-based thermochromic smart windows.

## 1 Introduction

With the ongoing development of industrialization, urbanization and modernization, global energy consumption has witnessed a significant increase. Building energy consumption now accounts for approximately 30% to 40% of total energy use, surpassing that of industry and transportation.[1,2] In 2021, energy-related $CO_2$ emissions from buildings reached 10 gigatons, the highest level ever recorded.[3] Notably, about 50% of building energy consumption is due to operations such as heating, ventilation, and air

[a] *Jiangsu Key Laboratory of Advanced Metallic Materials, School of Materials Science and Engineering, Southeast University, Nanjing 211189, China. E-mail: w69zhang@seu.edu.cn, zmsun@seu.edu.cn*
[b] *Molecular Science Institute, School of Chemistry, University of the Witwatersrand, Private Bag 3, Wits2050, Johannesburg 2000, South Africa*
[c] *Department of Materials Function and Design, Nagoya Institute of Technology, Gokiso-cho, Showa-ku, Nagoya, Aichi 466-8555, Japan*

Published on 18 September 2024. Downloaded by University of the Witwatersrand on 12/12/2024 3:02:43 PM.

conditioning (HVAC), and this consumption is projected to steadily increase over the next two decades.[4] Especially, air conditioning energy consumption stands out as a primary driver of this ongoing growth. The rapid increase in energy consumption and carbon emissions in the building sector has garnered global attention. Many countries increasingly recognize the pivotal role of buildings in achieving carbon neutrality. Windows are the key components of buildings, modulating daytime indoor lighting, aerating, allowing viewing, and decoration, while the heat exchange with the outdoor environment through windows is often contrary to that desired. Thus, windows are considered the least energy-efficient components of buildings,[5] for example, during during hot summers, strong sunlight penetrating through windows can generate excessive heat, leading to substantial cooling demands. Even in winter, significant heat loss occurs through windows. Therefore, improving window energy efficiency is essential for achieving energy savings in buildings.

Smart window technologies, such as electrochromic,[6,7] photochromic,[8,9] and thermochromic smart windows[10–13] have been proposed to modulate solar irradiation and indoor temperature by responding to specific stimuli-electricity, light and temperature, thereby achieving energy saving and emission reduction. However, electrochromic smart windows require an additional electric supply, leading to complicated device configurations and continuous energy consumption during the switching between coloring and bleaching states. The complexity and high cost of electrochromic technology also limit its large-scale application in buildings. Photochromic coatings rely on expensive physical vapor deposition and high-temperature processing, and their optical switching is strongly influenced by light intensity, making them susceptible to adverse weather conditions such as rain, fog, and clouds, which compromises their controllability. In contrast, thermochromic smart windows are considered the most promising candidate due to their ability to spontaneously adjust between transparent and opaque states in response to different ambient temperatures. Furthermore, the benefits of thermochromic windows include zero energy consumption, multi-band regulation, ease of implementation, cost-effectiveness, simplicity, and scalability, making them increasingly attractive for energy-saving applications in buildings.

Thermochromic materials serve as the key components of thermochromic smart windows. Considerable research has been dedicated to designing and synthesizing a variety of thermochromic materials with exceptional performance characteristics, including high luminous transmittance ($T_{lum}$), solar energy modulation ($\Delta T_{sol}$), suitable critical response temperatures ($\tau_c$) and durability. Thus, thermochromic materials have experienced rapid development. Through element doping,[14] the $\tau_c$ $VO_2$ has been significantly lowered, enabling the phase transition between the monoclinic and rutile. Additionally, some studies have achieved modulation of different solar radiation wavelength bands by integrating $VO_2$ with radiative cooling[15] and electrochromic technologies,[16] further enhancing its energy-saving performance. Hydrated thermochromic perovskite smart windows leverage reversible hydration and dehydration processes to switch between transparent and colored states.[17,18] A mask-inspired thermochromic perovskite



**Gang Xu**

*Gang Xu is a PhD candidate in Prof. ZhengMing Sun's group at the School of Materials Science and Engineering, Southeast University. His research focuses on the design of thermochromic and electrochromic materials and their applications in smart windows. He received his bachelor's degree from Nanjing Tech University in 2019.*



**Wei Zhang**

*Dr Wei Zhang is an associate professor in School of Material Science and Engineering at Southeast University. He obtained his MASc in Chemistry and PhD in Nanotechnology from the University of Waterloo. Since joining Southeast University in 2016, he has established the Surface Science and Bionanomaterials Laboratory, working on both fundamental and applied research to meet the growing need of nanotechnologies in advanced materials, e.g., multifunctional and smart hydrogels and aerogels, flexible energy storage devices or wearable electronic devices.*



**ZhengMing Sun**

*Prof. Sun received his PhD degree from the Institute of Metal Research (IMR), Chinese Academy of Sciences. He is currently a full professor in the School of Materials Science and Engineering, Southeast University. His research interests cover the research and development of metallic materials, intermetallic compounds, ceramics, and composites. Recently, he has been leading his group on the research and development of MAX phase materials, MXenes, and other low-dimensional materials, with a focus on application in energy storage and conversion. He has authored over 300 SCI indexed papers and applied over 40 patents.*


This journal is © The Royal Society of Chemistry 2024

Published on 18 September 2024. Downloaded by University of the Witwatersrand on 12/12/2024 3:02:43 PM.

smart window has also been developed, significantly improving environmental stability and advancing practical applications.[19] Thermochromic ionogels are synthesized by embedding ionic liquids (ILs) within specific 3D polymer networks,[20] utilizing the reversible phase separation between the ionic liquid and polymer. These ionogels exhibit excellent environmental and mechanical stability, along with self-healing and recyclability.[21] Additionally, a novel thermochromic material based on a salted polymer blend system has been reported, which can be easily coated onto various surfaces, allowing standard windows to be upgraded into smart windows.[22] Hydrogels, as emerging polymers, are characterized by three-dimensional networks of water and polymer chains.[23–25] The high water content in hydrogels provides them with a significant specific heat capacity, comparable to that of water.[26] This characteristic enables hydrogels to withstand substantial environmental fluctuations and maintain stable room temperatures effectively. Additionally, the water abundance in hydrogels facilitates transitions between hydrophilic and hydrophobic states, allowing for rapid switching between transparent and opaque states. Moreover, by adjusting the composition and structure of the hydrogel, its critical transition temperature ($\tau_c$) can be tailored to suit various environmental conditions and operational needs. Specific hydrogel systems, like poly(*N*-isopropylacrylamide) (PNIPAm)[27] and hydroxypropyl cellulose (HPC),[28] demonstrate significantly higher luminous transmittance than conventional thermochromic materials such as $VO_2$ and perovskite. The significant difference in transparency between the transparent and opaque states allows the hydrogels to achieve effective solar modulation. Table 1 presents a comparison of the most investigated thermochromic smart windows, including $VO_2$, perovskite, and hydrogels. Owing to their excellent thermochromic performance and various benefits, thermochromic hydrogels have captured significant attention in the field of energy-saving smart windows.

Over the past three years, a large number of review articles have been reported on thermochromic smart windows. Some of these reviews focus on specific thermo-responsive materials, such as $VO_2$,[10,14,29–31] perovskites,[18,32,33] and liquid crystals,[34] while others cover a broad range of thermochromic materials.[1,35–37] There still no reviews specifically focus on thermochromic hydrogel-based smart windows. Thus, comprehensive investigations into thermo-responsive hydrogel-based smart windows are necessary, which will enhance the understanding of the polymerization strategies, chromic mechanisms, emerging research trends, and foster the development of these hydrogels. This review begins with an exploration of fabrication strategies and thermochromic mechanisms in various thermochromic hydrogels, providing insights from a molecular perspective rather than the conventional phase separation. It then discusses recent advancements in the responsiveness, stability, and energy-saving performance of thermochromic hydrogels, including thermo-electro and thermo-photo dual-responsiveness, tunable critical temperatures, freezing resistance, and the integration of smart windows with radiative cooling and power generation technologies (Fig. 1). Finally, we provide a perspective on future research directions in this field, highlighting the challenges faced by thermochromic hydrogel smart windows. We hope this review offers new insights for their design, development and practical applications.

## 2 Fabrication and chromic mechanisms of thermochromic hydrogels

In 2014, Long *et al.*[27] initially fabricated a thermochromic smart window *via* injecting a precursor solution of PNIPAm between two glass panels and conducting *in situ* polymerization. The as-prepared smart window demonstrated an unprecedented good combination of $T_{lum}$, $\Delta T_{sol}$, and suitable $\tau_c$, marking the first hydrogel-based thermochromic smart window. Subsequently, various thermochromic hydrogels including HPC,[28,38] methylcellulose (MC),[39] poly(*N*-vinylcaprolactam) (PNVCL),[40,41] polyhydroxy propyl acrylate (PHPA),[42] polyvinyl butyral (PVB),[43] sodium dodecyl sulfate (SDS)-derived hydrogels,[43–47] and hybrid systems like PNIPAm/HPC,[48,49] PNIPAm/hydroxypropylmethyl cellulose (HPMC),[50] HPC/PAA,[51] PNIPAm/SDS/PAAm[52,53] and polyelectrolyte hydrogels,[54,55] zwitterionic hydrogels,[56] PNIPAm hydrogel microgels,[57] P(NIPAm-*co*-AA)-based chain/microparticle hybrids,[58] and solid–liquid switchable PNIPAm hydrogels[59] have been proposed.

The chromic mechanism of thermochromic hydrogels has long been attributed to phase separation between the hydrogel network and water, induced by its lower critical solution

Table 1 A brief comparison of most investigated $VO_2$, perovskite, and hydrogel thermochromic smart windows

| Materials | Chromic mechanisms | Representative materials | Advantages | Limitations |
|---|---|---|---|---|
| $VO_2$ | Phase change transition | — | Good stability, fast switching speed | Relatively high $\tau_c$, poor $T_{lum}$ and $\Delta T_{sol}$, unfavorable color and the potential toxicity after oxidization |
| Perovskite | Hydration/dehydration or phase transitions or lattice expansion | $MA_4PbI_6{\cdot}H_2O$<br>H-$MAPbI_3$<br>H-$MAPbI_{3-x}Cl_x$ | Numerous structures, colorful appearance, and have potential to integrate with power generation | Poor stability, mainly regulate near-infrared wavelength, and multistep processing |
| Hydrogel | Phase separation | PNIPAm<br>HPC<br>SDS-derived hydrogels | Good $T_{lum}$ and $\Delta T_{sol}$, facile fabrication and large-scale availability | Concerning stability and high cost |

Published on 18 September 2024. Downloaded by University of the Witwatersrand on 12/12/2024 3:02:43 PM.

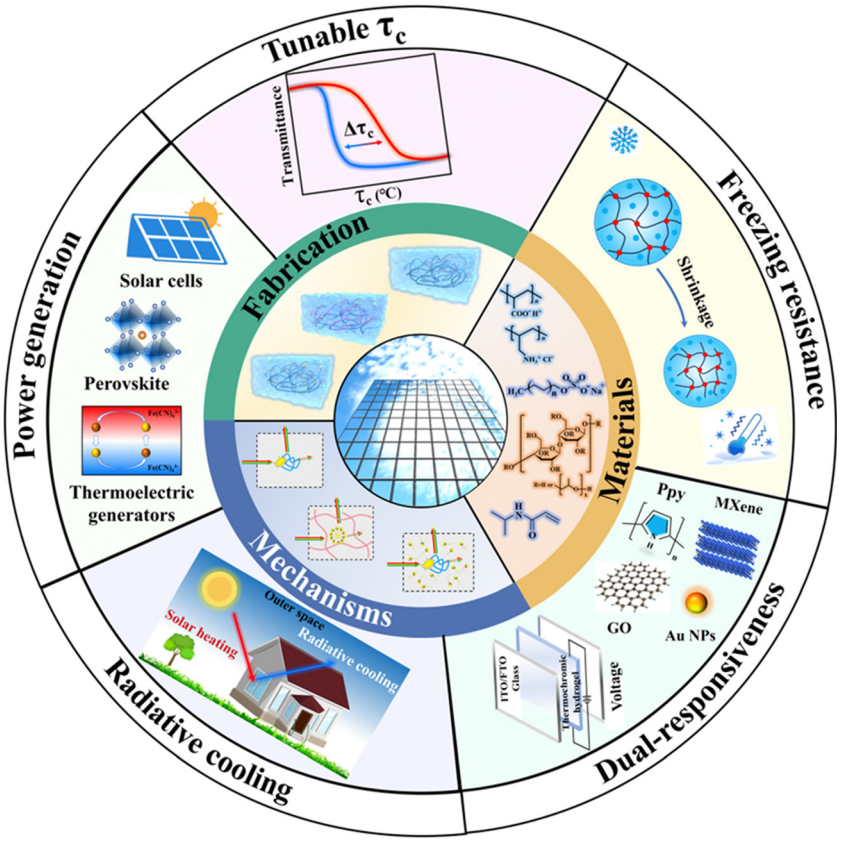



Fig. 1 Illustration of fabrication, mechanisms, and advancing trends of thermochromic hydrogel-based smart windows.

temperature (LCST). This phase separation causes multiple scattering of incident sunlight within the hydrogel network, resulting in a macroscopically opaque state.[60] However, this explanation does not universally apply to the diverse range of current thermochromic hydrogels, as phase separation varies among different types. The conformation of polymer chains and the aggregation states of thermo-responsive units within the hydrogel network differ fundamentally around the critical transition temperature. Therefore, it is necessary to understand the chromic mechanism of thermochromic hydrogels from a molecular perspective. Here, we categorize thermochromic hydrogels into three main types based on their chromic mechanisms: chain segment coil–globule transition hydrogels, micelle reversible aggregation and dissociation thermochromic hydrogels, and hybrid mechanism thermochromic hydrogels. Table 2 summarizes the thermochromic mechanisms and performance of typical hydrogels.

### 2.1 Coil–globule transition of polymer chains

PNIPAm hydrogels, typically synthesized through free radical polymerization with the initiator and crosslinker[64] (Fig. 2a), exhibit a characteristic coil–globule transition mechanism in thermochromic polymer chains. PNIPAm contains amide (–R–C(═O)–$NH_2$) and isopropyl moieties (($(CH_3)_2$CH–), and has a LCST of ~32 °C in water. Below the LCST, hydrogen bonding between hydrophilic amide groups and water molecules counteracts the hydrophobic interactions among isopropyl groups, preventing the PNIPAm chain from collapsing. When the temperature exceeds the LCST, the hydrogen bonds weaken while hydrophobic interactions strengthen, resulting in an entropy-driven phase separation.[57,60] The PNIPAm chains then dehydrate and aggregate into a dense globular form, causing significant scattering of incident sunlight (Fig. 3a). HPC,[28] a water-soluble cellulose derivative, contains both hydrophilic hydroxyl groups and hydrophobic hydroxypropoxy groups. It readily dissolves in water or salt solutions, enabling the fabrication of thermochromic HPC hydrogels, which undergo a coil-to-globule transition in response to temperature changes. Similarly, other hydrogels, such as MC, PNVCL, PVB, and PHPA, also exhibit coil–globule transitions. Polyelectrolyte hydrogels,[55] an emerging type of thermochromic hydrogel, are formed by the complexation of oppositely charged polyelectrolytes in aqueous solutions. These hydrogels undergo reversible hydration and dehydration during the thermo-responsive process, when the temperature is higher than $\tau_c$, polyelectrolyte complexes aggregate into hydrophobic domains, leading to obvious phase separation. This behavior demonstrates a chromic mechanism similar to the coil–globule transition.

### 2.2 Aggregation and dissociation of micelles

Current thermochromic smart windows based on LCST behavior can achieve solar regulation and energy saving by

 This journal is © The Royal Society of Chemistry 2024

Published on 18 September 2024. Downloaded by University of the Witwatersrand on 12/12/2024 3:02:43 PM.

Table 2 Thermochromic mechanisms and performance of typical hydrogels

| Materials | Chromic mechanisms | Characteristics | $T_{lum}$ (%) | $\Delta T_{sol}$ (%) | $\tau_c$ (°C) | Ref. |
|---|---|---|---|---|---|---|
| PNIPAm | Coil–globule transition of polymer chains | First PNIPAm thermochromic smart window | 70.7 | 25.5 | 32 | 27 |
| PNIPAm-AEMA | | Microparticles, with broadband light management, great scalability and stability | 87.2 | 81.3 | 32 | 57 |
| PNIPAm-DMAA | | Adjustable $\tau_c$, strong solar modulation, 3D printing | 91.3 | 88.84 | 32.5–43.5 | 61 |
| PNIPAm-PAM | | Precisely predict and fabricate the hydrogel with the desired, broad $\tau_c$ range | 95.0 | — | 32–54 | 62 |
| HPC | | First HPC thermochromic smart window | 67.4 | 25.7 | 30–42 | 28 |
| PNIPAm/HPC | | Fast response time, anti-freezing and anti-drying | 80.7 | 64.5 | 29 | 48 |
| HPC/PAA | | Tunable $\tau_c$ by adjusting pH, excellent stability | 90.1 | 47.5 | 10–44 | 51 |
| Methylcellulose (MC) | | Wide range of $\tau_c$ tunability, excellent optical and thermal properties | 86 | 53 | 34–72 | 39 |
| PNVCL | | Fast reversible response, thermo-electrical dual response | 88 | — | 34 | 40 |
| Polyhydroxy propyl acrylate (PHPA) | | Adjustable $\tau_c$, fast optical response, favorable stability | 93.7 | 81.1 | 12–34 | 42 |
| Polyvinyl butyral (PVB) | | Frost resistance, isochoric phase transition, recyclability, and tough mechanics | ~90 | 80.8 | 28 | 43 |
| PAH-PAA-CPDs | | Rapid transition, anti-freezing ability, self-healing capability | 98.7 | 89.3 | 24.2 | 55 |
| PAAm/SDS/PTH/LiCl | Aggregation and dissociation of SDS micelles | Thermo-electrical dual response, favorable flexibility | 88.3 | — | 28–35 | 44 |
| PAAm/SDS/EG | | Wide $\tau_c$ range, finely tune the response temperature | 98.83 | — | 6–75 | 45 |
| PAAM/SDS/$Li^+$/$Na^+$/$K^+$ | | Excellent solar modulation ability, dual responsiveness, tunable $\tau_c$, easy to fabricate mechanical flexibility | 99.05 | 33.42 | 20–50 | 63 |
| PNIPAm/SDS/PAAm | PNIPAm/SDS hybrid chromic mechanisms | With two critical transition temperatures | 91.31 | 76.34/76.75 | 9.5–50 | 53 |
| PNIPAm/SDS/PAAm | | A reversible three-stage transition of opaque–transparent–translucent | 80.3 | 72.9/42.7 | 16.2–32.4 | 52 |

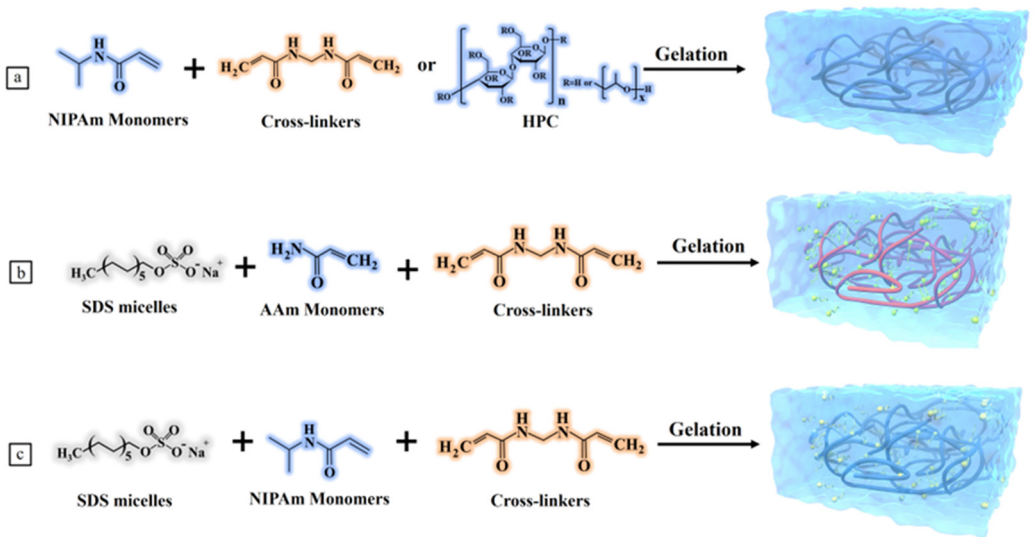



Fig. 2 The fabrication schematics of three types of thermochromic hydrogels. (a) Thermal-responsive monomer-based hydrogels are formed *via* free radical polymerization or simple dissolution methods. (b) SDS-derived thermochromic hydrogels involve introducing SDS micelles into a solution of hydrogel precursors, followed by polymerization using free radical polymerization. (c) Hybrid thermochromic hydrogels are synthesized using a classic one-pot method.

modulating solar transmission at the cost of visibility at higher temperature,[56] ignoring the indoor lighting required during the daytime and the privacy protection in the nighttime. In contrast, the chromic mechanism of thermochromic hydrogels derived from SDS exhibits an opposite pattern: transparency increases with rising temperature, a characteristic of upper critical solution temperature (UCST) behavior,[65] thereby providing sufficient visibility during the day and privacy protection at night.

SDS, as an anionic surfactant, is commonly dissolved in the precursor solution of hydrogels, where it forms SDS micelles that serves as the thermo-responsive units.[63,66] The hydrogel with high transparency, which maintains high transparency,

Published on 18 September 2024. Downloaded by University of the Witwatersrand on 12/12/2024 3:02:43 PM.

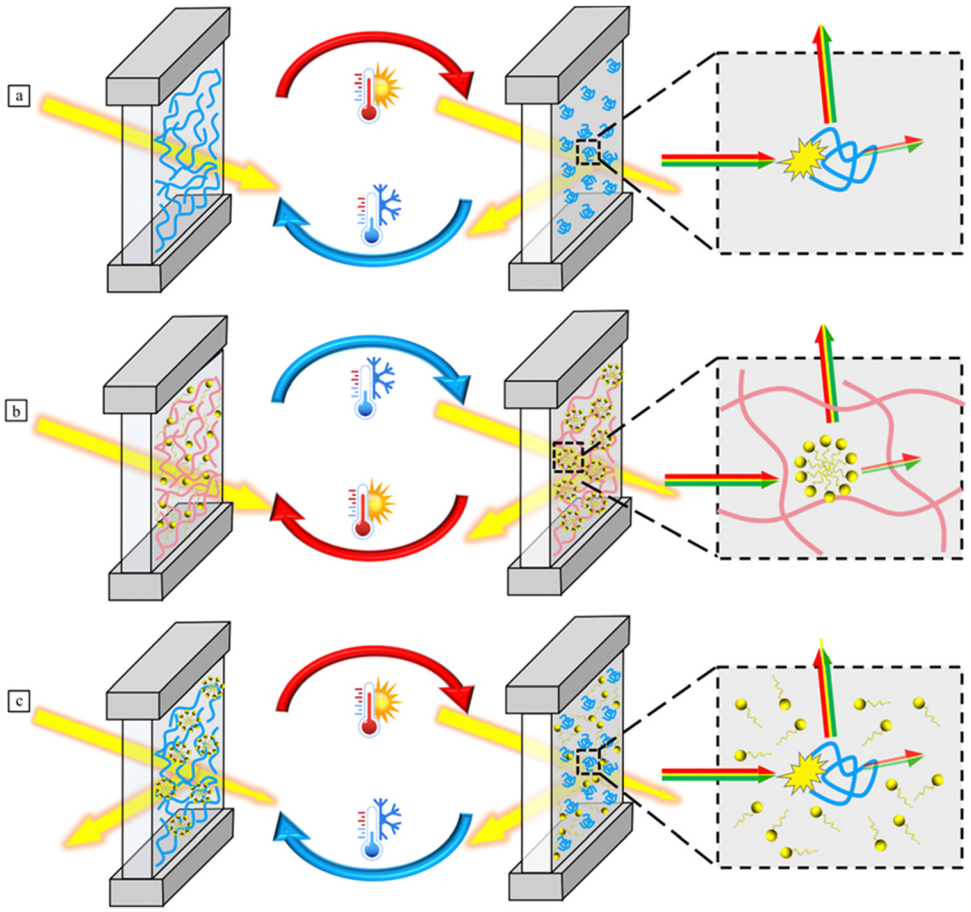



Fig. 3 Thermochromic mechanisms of the three main types of thermochromic hydrogels: (a) coil–globule transition of polymer chains: as the temperature rises above $\tau_c$, PNIPAm chains dehydrate and aggregate into a tightly packed globular conformation, causing strong scattering of incident sunlight. (b) Aggregation and dissociation of SDS micelles: below the $\tau_c$, dissociated SDS micelles within the hydrogel's three-dimensional network spontaneously aggregate, increasing in size and leading to light blockage. (c) Hybrid hydrogels: these contain two types of thermal-responsive units, resulting in multiple thermochromic characteristics.

acts as the matrix in which the SDS micelle can be confined in the three-dimensional cross-linking network of the hydrogel (Fig. 2b). The size of SDS micelles is temperature-dependent. Below the $\tau_c$, dissociated SDS micelles in the hydrogel's three-dimensional network spontaneously aggregate and form micellar clusters, leading to light blockage and opacity. Upon heating, the micellar clusters dissolve and disperse within the hydrogel due to the disruption of H-bonds, allowing incident light to pass through and rendering the hydrogel transparent for indoor illumination (Fig. 3b). Inorganic salts, such as LiCl, NaCl, and KCl, especially cation, play a crucial role in adjusting the critical micelle concentration (CMC) of SDS micelles and the $\tau_c$ in these hydrogel systems. Similarly, other surfactants, including sodium dodecyl sulfonate (SLS), sodium dodecyl benzene sulfonate (SDBS), magnesium dodecyl sulfate ($Mg(DS)_2$), and hexadecylpyridinium bromide (HPB)[67] can also exhibit thermochromic properties.

### 2.3 Hybrid chromic mechanism

The last category of thermochromic hydrogels combines features from both the first and second types, with one of the most prominent examples being PNIPAm/SDS hydrogels.[52,53] These hydrogels are typically synthesized using a classic one-pot method where NIPAm monomer, SDS, inorganic salts, initiators, and crosslinkers are mixed and dissolved together (Fig. 2c).

Hybrid thermochromic hydrogels exhibit a dual thermochromic mechanism involving two types of thermal-responsive units, often demonstrating both LCST and UCST characteristics, resulting in two distinct $\tau_c$ (Fig. 3c). At lower temperatures, SDS micelles spontaneously aggregate within the hydrogel, scattering sunlight and rendering it opaque. This thermochromic effect is primarily driven by SDS. As the temperature increases, these micellar clusters dissolve, causing the hydrogel to become transparent. Upon further temperature elevation, the hydrogel undergoes a coil–globule transition where PNIPAm contributes to opacity, resulting in the hydrogel becoming opaque once again. In general, such mixed hydrogels undergo an opaque–transparent–opaque process as temperature varies, exhibiting a range of thermochromic effects suitable for diverse applications. For instance, they can provide privacy at lower temperatures, allow for natural lighting at intermediate temperatures, and block solar

 This journal is © The Royal Society of Chemistry 2024

Published on 18 September 2024. Downloaded by University of the Witwatersrand on 12/12/2024 3:02:43 PM.

radiation at higher temperatures, thereby helping to reduce indoor temperature.

### 2.4 Other chromic mechanisms

Unlike the previously mentioned chromic mechanisms, zwitterionic hydrogels demonstrate a distinct mechanism. These hydrogels are formed by ionic bonding between oppositely charged units within the polymer backbone chains and can be synthesized through photo-cross-linking[54] or one-step radical copolymerization.[56] They display UCST behavior, which occurs due to the reversible phase-separation of water and polymer chains. At lower temperatures, strong intermolecular interactions among the polymer chains result in the formation of polymer-rich regions, leading to an opaque hydrogel. When the temperature reaches the $\tau_c$, the balance between the dissolution and insolubilization of polymer chains is achieved. As the temperature increases, these strong interactions are disrupted, causing the polymer chains to uniformly disperse in the water, thus resulting in a transparent hydrogel.

## 3 Advancements in thermochromic hydrogel smart windows

Over the past decade, thermochromic hydrogel-based smart windows have witnessed rapid development, not only a higher $T_{lum}$ and $\Delta T_{sol}$, but also advancements in responsiveness, stability, and energy-saving performance of hydrogel-based thermochromic smart windows, which are crucial for practical application.

### 3.1 Advancements in responsiveness

Thermochromic hydrogels can spontaneously switch between transparent and opaque states in response to varying ambient temperatures. However, their single thermal responses, monochromatic color (opaque: white, transparent: colorless), and fixed $\tau_c$ limit applicability across diverse scenarios and regions.[68] To overcome these limitations, significant efforts have been made to develop hydrogels with dual-responsiveness and tunable $\tau_c$.

#### 3.1.1 Dual-responsiveness

*Thermo-electro dual-responsiveness.* The passive response characteristic makes the thermochromic hydrogel realize the state switch only when the temperature is higher than the $\tau_c$. While the passive adjustment of transparency based on ambient temperatures may hinder the application of thermochromic smart windows in scenarios like privacy windows, where active control is essential. Electrothermal devices have been developed to actively control thermo-responsive smart windows by integrating thermochromic hydrogels with transparent conductive substrates such as indium tin oxide (ITO) glasses,[44,69,70] fluorine-tin oxide (FTO) glasses,[40,41] and ZnO/Ag/ZnO multilayer films.[71] These substrates heat thermochromic hydrogels through Joule heating when a voltage is applied. Zhong *et al.*[72] developed a thermo-electro dual-responsive smart window using two FTO glass panels, with a PNIPAm hydrogel encapsulated within. Applying a 5 V voltage to this 25 mm × 25 mm × 2.2 mm window achieved a $\Delta T_{sol}$ of 26.51% and rapid response speed.

The integration of thermochromic with electrochromic properties is also receiving increasing attention. A conventional electrochromic smart window typically consists of at least five layers: two transparent conductive electrodes, an electrochromic layer, an electrolyte layer, and an ion storage layer.[73] By introducing the thermochromic hydrogels into the electrochromic smart windows, these hydrogels not only fulfill the role of electrolyte and ion storage but also endow thermochromic capabilities with electrochromic smart windows. This integration simplifies the structure, typically reducing it to a four-layer configuration: an electrochromic layer, thermochromic hydrogel, and two transparent conductive electrodes. As shown in Fig. 4a, Wang *et al.*[74] present a thermo-electrochromic dual-responsive smart window by injecting PNIPAm hydrogel containing $LiClO_4$ between two FTO glass electrodes, one of which is coated with an electrochromic $WO_3$ layer. In this device, the electrochromic layer changes colors under an electrical field, while the electrolyte induces transmittance changes controlled by temperature. This setup allows for four operational states (Fig. 4b): bleached/transparent, colored/transparent, bleached/opaque, and colored/opaque, catering to diverse application needs. To further simplify the structure of the electrothermochromic smart window, Urain *et al.*[41] introduced an all-in-one hydrogel for thermo-electrochromic applications. This innovation integrates electrochromic viologens into thermochromic PNIPAm hydrogel, resulting in a dual-responsive smart window with just three layers: two transparent FTO electrodes and a PNIPAm-viologen hydrogel.

The thermo-electro dual-responsive smart window integrates both passive and active chromic capabilities. By leveraging the Joule heating from a transparent conductive layer when voltage is applied, the thermochromic hydrogel can transition from a transparent to an opaque state below $\tau_c$ with the cost of energy consumption.[36] Some systems also offer multiple operational states, addressing the limitation of single-color display.

*Thermo-photo dual-responsiveness.* While active control can be achieved through the electrothermal method, it requires continuous electricity consumption to maintain the desired temperature. An alternative approach utilizes photothermal materials that respond to optical stimuli by generating heat through absorption to endow the thermochromic hydrogels with an additional stimulus. Enhancing this effect involves integrating thermochromic materials with high-absorbance photothermal materials (Fig. 4c), such as graphene oxide (GO),[76] cesium tungsten bronze nanorods ($Cs_{0.32}WO_3$),[77] antimony-tin oxide (ATO),[75,78] or materials with localized surface plasmon resonance (LSPR) like gold nanoparticles (Au NPs)[25,79,80] (Fig. 4d).

Tian *et al.*[81] developed a fully autonomous photosensitive smart window that responds to sunlight intensity and ambient temperature by incorporating polydopamine particles (PDAPs) into thermochromic PNIPAm hydrogels. PDAPs absorb infrared rays from the sun, converting them into localized heat, which

Published on 18 September 2024. Downloaded by University of the Witwatersrand on 12/12/2024 3:02:43 PM.

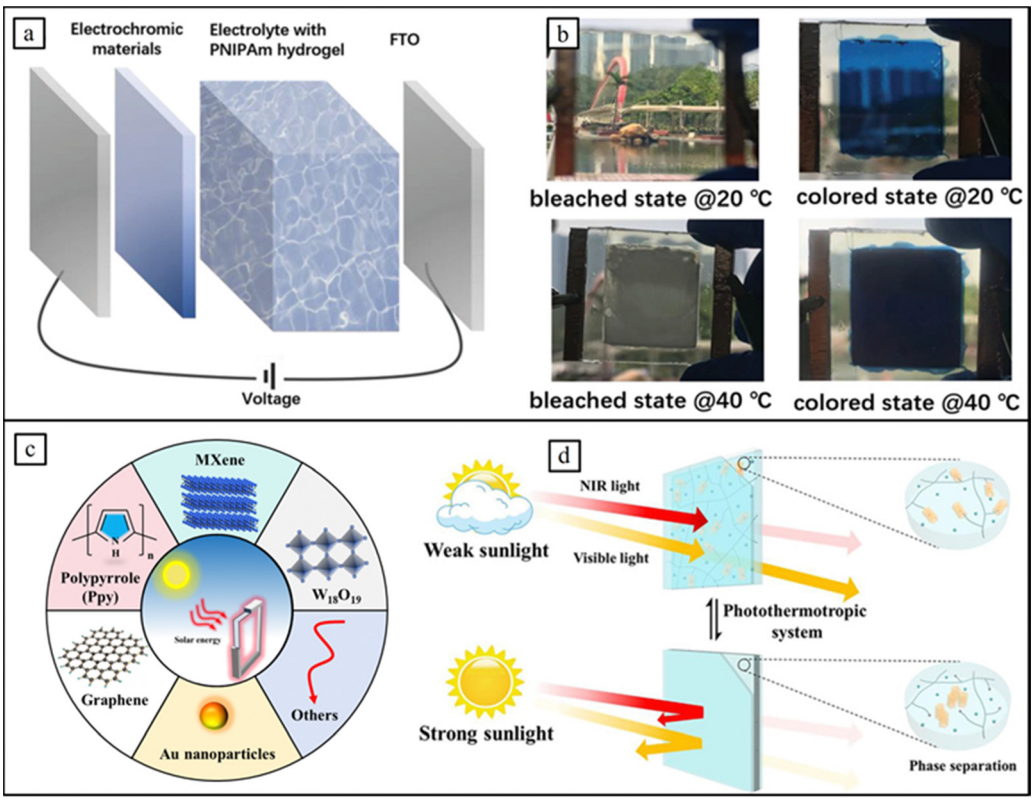



Fig. 4 Dual-responsive thermochromic hydrogels. (a) The structure of the thermo-electrochromic dual-responsive smart windows containing two FTO conductive glasses, an electrochromic layer, and thermochromic PNIPAm electrolyte. (b) Photographs illustrating the smart window in four distinct states: bleached/transparent, colored/transparent, bleached/opaque, and colored/opaque. (a) and (b) Reproduced with permission from ref. 74. Copyright 2019, Wiley-VCH. (c) Various photo-thermal materials are incorporated with thermochromic hydrogels. (d) Illustration of the photo-thermal effect and the thermochromic switching process. Reproduced with permission from ref. 75. Copyright 2018, Wiley-VCH.

raises the temperature of the PNIPAm above the $\tau_c$. Polypyrrole (Ppy),[82] a π-conjugated polymer, can efficiently convert solar energy into heat, leading to a rapid temperature increase. Benefiting from the Ppy's photothermal conversion, the PNIPAm/Ppy hydrogel exhibits a significantly faster phase transition compared to the pure PNIPAm hydrogel. Recently, MXene,[83,84] a 2D nanomaterial known for its superior photothermal conversion, thermal conductivity, and favorable dispersibility, has also gained prominence for introduction into thermochromic hydrogels to achieve thermo-photo dual-responsiveness. $W_{18}O_{49}$ has also been utilized for its responsiveness to strong UV light and its ability to block most NIR light in its colored state. Tao *et al.*[85] propose a reversible photothermochromic hybrid smart window combining photochromic $W_{18}O_{49}$ and thermochromic PAM–PNIPAm hydrogels. This window achieves graded and dual-band sunlight control. As solar irradiation increases, the window gradually attenuates NIR light while maintaining high $T_{lum}$. Upon reaching maximum solar irradiation, the ambient temperature rises to $\tau_c$, causing the hydrogel to block full-spectrum sunlight.

By incorporating photothermal materials into the 3D network of thermo-responsive hydrogels, solar energy is converted into heat through a photothermal effect, raising the hydrogel's temperature to $\tau_c$ and facilitating its phase transition. This approach also enhances the response speed of the hydrogel. However, it is important to note that the inclusion of photothermal materials may reduce the hydrogel's overall transmittance.

**3.1.2 Tunable critical transition temperatures.** Most thermochromic smart windows are constrained by a fixed $\tau_c$, restricting their adaptability across different climates and regions. To address this limitation, several strategies have been proposed, including copolymerization and incorporating alcohol solvents or inorganic salts. These approaches enable a broad range of $\tau_c$ and precise regulation of $\tau_c$ in thermochromic hydrogels.

*Modulation of hydrogel networks.* The co-polymerizing strategy demonstrates significant potential in enhancing hydrogel network stability and enabling tunable $\tau_c$.[86] Introducing a second monomer disrupts the hydrogen bond network, and the alteration of $\tau_c$ depends on the properties of this monomer. For example, copolymerizing acrylamide (AAm),[62] a hydrophilic monomer, with PNIPAm increases $\tau_c$. The hydrophilic amide groups in AAm form hydrogen bonds with water molecules, which interact with the hydrophobic isopropyl groups of PNIPAm, thereby weakening overall hydrophobic interactions and causing thermochromism to occur only at higher temperatures. Another similar monomer, *N*,*N*-dimethylacrylamide (DMAA)[61] (Fig. 5a), when copolymerized with NIPAm, forms random

 This journal is © The Royal Society of Chemistry 2024

Published on 18 September 2024. Downloaded by University of the Witwatersrand on 12/12/2024 3:02:43 PM.

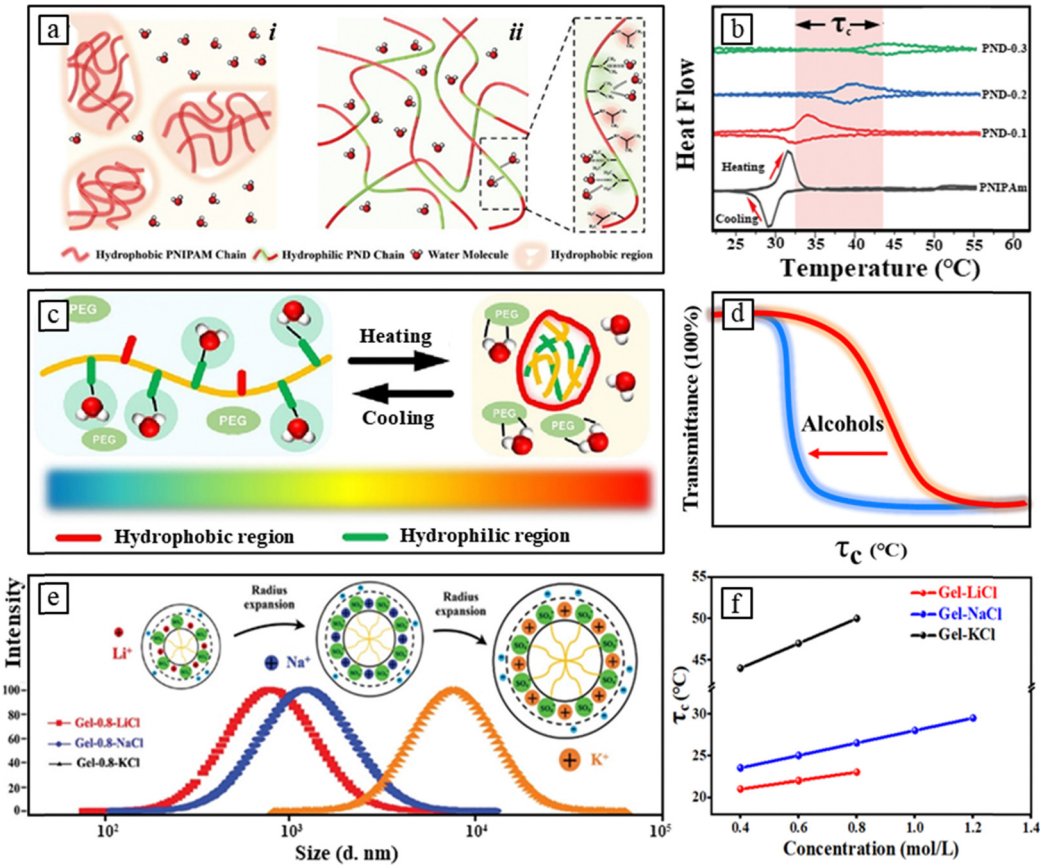



Fig. 5 Thermochromic hydrogels with a tunable thermochromic transition temperature. (a) The schematic illustrates (i) PNIPAM and (ii) P(NIPAM-*co*-DMAA) (PND) hydrogel structures. (b) DSC curves of PND hydrogels with varying amounts of DMAA. (a) and (b) Reproduced with permission from ref. 61. Copyright 2023, Wiley-VCH. (c) Schematic showing thermochromism on heating and cooling after incorporating with poly-ethylene glycol (PEG). Reproduced with permission from ref. 87. Copyright 2024, Elsevier. (d) The $\tau_c$ of PNIPAm-based hydrogels can be significantly reduced by alcohols and their derivatives. (e) Dynamic light scattering (DLS) results showing average micelle sizes for Gel-0.8-LiCl, Gel-0.8-NaCl, and Gel-0.8-KCl precursor solutions at 25 °C, alongside their micelle structures. (f) $\tau_c$ of the hydrogels with different types and concentrations of inorganic salts. (e) and (f) Reproduced with permission from ref. 63. Copyright 2022, Wiley-VCH.

copolymer P(NIPAm-*co*-DMAA) (PND) hydrogels with adjustable $\tau_c$ values ranging from 32.5 to 43.5 °C (Fig. 5b). In contrast, acrylic acid (AA), which contains a carboxyl group, enhances copolymer–water interactions and decreases $\tau_c$. Zhang *et al.*[51] fabricated an HPC/PAA hydrogel smart window, reducing its $\tau_c$ from 44 to 10 °C. Additionally, hydrogels containing two thermo-responsive units also influence $\tau_c$. Yu *et al.*[53] developed a hybrid thermochromic smart window by incorporating SDS micelles into a PNIPAm hydrogel, possessing simultaneous UCST and LCST. This window transitions from opaque (SDS-led) to transparent as the temperature rises, and then turns opaque again (PNIPAm-led) at higher temperatures, offering a multi-stage optical modulation.[52,67]

*Low-polarity alcohol solvents.* The addition of alcohol solvents decreases the $\tau_c$ of thermochromic hydrogels by reducing the overall polarity of the solvent system. Alcohol solvents, which have lower polarity compared to water, weaken the hydrogen bonds between the hydrogel and solvent molecules, thereby lowering the temperature at which these bonds break. Consequently, increasing the concentration of alcohol solvents decreases the $\tau_c$ of the hydrogel. Jiang *et al.*[87] developed smart windows based on organohydrogels by polymerizing NIPAm in a polyethylene glycol-water binary solvent system through *in situ* free radical polymerization (Fig. 5c and d). The $\tau_c$ was sharply reduced to below 10 °C, attributed to the strengthened hydrogen bonding between the mediums, which affected the interaction between copolymer chains and water molecules. Similarly, Li *et al.*[88] introduced glycerol into the hydrogel, and with an increasing weight fraction of glycerol from 0 to 30 wt%, the $\tau_c$ decreased from 31.0 to 16.0 °C. Additionally, the addition of a small amount of ethanol can also further reduce the attraction between PNIPAm and water, as well as the surface tension of water, thereby lowering the $\tau_c$ to 28 °C.[89]

*Inorganic/organic salts.* The introduction of inorganic salts is a widely employed approach to modify the $\tau_c$ of thermochromic hydrogels. Inorganic salts such as NaF, NaCl, NaBr, NaI,[90] $Na_2SiO_3$,[91] $Na_2SO_4$,[39,62] and KCl[60] increase the ionic strength of the solution, thereby affecting the hydrogen bond interactions between PNIPAm molecules and water. These salts form a hydration layer around water molecules, reducing their activity

Published on 18 September 2024. Downloaded by University of the Witwatersrand on 12/12/2024 3:02:43 PM.

and altering their interaction with PNIPAm, which leads to a decrease in $\tau_c$. This effect is observed in thermochromic HPC hydrogels as well. For example, Yang *et al.*[28] demonstrated that the $\tau_c$ of an HPC hydrogel-based thermochromic material can be adjusted by adding NaCl, making it suitable for various climates. Increasing the NaCl concentration from 0.5 to 5 wt% decreased the $\tau_c$ from 42 to 30 °C.

In contrast, SDS-based thermochromic hydrogels exhibit distinct mechanisms for regulating $\tau_c$.[63] Higher concentrations of inorganic salts result in increased absorption of cationic ions into SDS micelles, potentially enlarging their size and enhancing aggregation, thereby raising $\tau_c$ (Fig. 5e and f). Additionally, the $\tau_c$ can vary significantly, typically ranging from 20 to 50 °C, depending on the cation radius of the metal atoms and the concentrations of inorganic salts. Ionic liquids, an emerging class of substances, also influence the $\tau_c$ of thermochromic hydrogels similarly to inorganic salts.[92]

The $\tau_c$ of thermochromic hydrogels now covers a broad range, from 6 °C[45] to 72 °C,[39] making them suitable for various climates and regions. However, blindly reducing the $\tau_c$ can cause the smart window to transition from transparent to opaque prematurely, leading to increased artificial lighting requirements.

### 3.2 Advancements in stability

Thermochromic hydrogels, due to their high-water content, exhibit poor stability to low temperatures and are prone to freezing. The free water within the hydrogel's three-dimensional network undergoes freeze, leading to irreversible structural damage and a significant decrease in thermochromic properties.[93,94] While previous research has focused on enhancing thermochromic performance, such as $T_{lum}$ and $\Delta T_{sol}$, the environmental stability, particularly anti-freezing capability, crucial for practical applications, has been overlooked.[88] The water molecules in a hydrogel come in three forms: free water, weakly bound water, and unfrozen water. The free water is prone to freezing and the key to improve the anti-freezing ability is to increase interactions between water molecules and the polymer network to reduce the presence of free water. Several strategies have been proposed by altering the composition of free water, such as incorporating glycol/ethylene glycol, ionic liquids, or developing composite thermochromic hydrogels.

**3.2.1 Glycerol/ethylene glycol.** The addition of alcohol solvents to the hydrogel network reduces the freezing point of resulting hydrogels due to the entropic effect and disruption of the three-dimensional hydrogen bond network, thereby decreasing the number of free water molecules.[95] Li *et al.*[88] developed a new physically crosslinked thermochromic smart window by incorporating NIPAm into a glycerol–water (GW) binary solvent system (Fig. 6a), achieving a high $T_{lum}$ of 90%, $\Delta T_{sol}$ of 60.8%, and remarkable freezing tolerance ($\sim -18$ °C). Density functional theory (DFT) analysis indicated that the interaction energy of the glycerol–water system is lower than that of the water–water system, suggesting greater stability of hydrogen bonding in glycerol–water. Consequently, the introduction of glycerol lowers the freezing point of the non-covalently crosslinked PNIPAM-GW hydrogel. Similarly, Wang *et al.*[96] developed PNIPAm/ethylene glycol (PNDE) hydrogels with adjustable and excellent freezing resistance by incorporating ethylene glycol. This incorporation resulted in freezing points of 0 °C ($PND_{25}E_0$), −8 °C ($PND_{25}E_{20}$), −27 °C ($PND_{25}E_{40}$), and −39 °C ($PND_{25}E_{50}$) as the ethylene glycol content increased (Fig. 6b). The addition of ethylene glycol significantly enhanced the hydrogel's freezing resistance by forming strong hydrogen bonds with water, thereby preventing freezing.

**3.2.2 Ionic liquids.** Ionic liquids have attracted considerable attention from researchers due to their distinctive characteristics, such as low vapor pressure, high chemical stability, excellent ion conductivity, and extreme temperature tolerance[97] (Fig. 6c). A thermochromic hydrogel, consisting of poly(oligoethylene glycol methyl ether methacrylate-*co*-acrylic acid) (P(OEGMA-*co*-AA)) and hydrated ionic liquid (HIL),[98] is synthesized through one-pot photopolymerization. The HIL, is integrated into the hydrogel matrix, effectively reducing the freezing point of water (to −15 °C) and enhancing the hydrogel's resistance to freezing.

**3.2.3 Hybrid thermochromic system.** Water molecules are known for their propensity to form strong hydrogen bonds with hydrophilic groups, leading to robust interactions and a significant depression of the freezing point. Modifying the hydrogel network can disrupt the water structure and inhibit ice nucleation. Feng *et al.*[48] conducted research where they incorporated HPC fibers into a PNIPAm hydrogel matrix (Fig. 6d), observing that increasing the HPC content lowered the freezing point of the PNIPAm–HPC hydrogel. This effect is attributed to hydrogen bonding interactions between HPC and PNIPAm. DFT simulations further supported these findings, revealing that the interaction energy between water and HPC is lower than that between water molecules themselves. Consequently, HPC tends to form hydrogen bonds with water molecules, disrupting the tetrahedral hydrogen bond network and thereby preventing water crystallization at low temperatures.

### 3.3 Advancements in energy-saving performance

Thermochromic hydrogel (LCST-type) smart windows are engineered to regulate solar radiation by dynamically adjusting their transmittance, thereby reducing solar transmission during hot conditions and maximizing solar transmission during cold conditions, resulting in a high $\Delta T_{sol}$. While $\Delta T_{sol}$ is often considered a key indicator of the energy-saving performance of thermochromic materials, this perspective is incomplete. The solar modulation value primarily accounts for the transmittance of ultraviolet, visible, and near-infrared bands (0.2–2.5 μm), but it overlooks the significance of reflectivity within this range and the material's emissivity – both of which are critical to the overall energy efficiency of smart windows. Furthermore, thermochromic smart windows typically focus on regulating solar transmission and indoor temperature but rarely consider utilizing the windows as a medium to harness solar energy and convert it into electricity for building use, thereby achieving greater energy-saving performance. This section systematically summarizes the integration of thermochromic technology with radiative cooling to simultaneously regulate transmittance, reflectance, and emissivity, as well

 This journal is © The Royal Society of Chemistry 2024

Published on 18 September 2024. Downloaded by University of the Witwatersrand on 12/12/2024 3:02:43 PM.

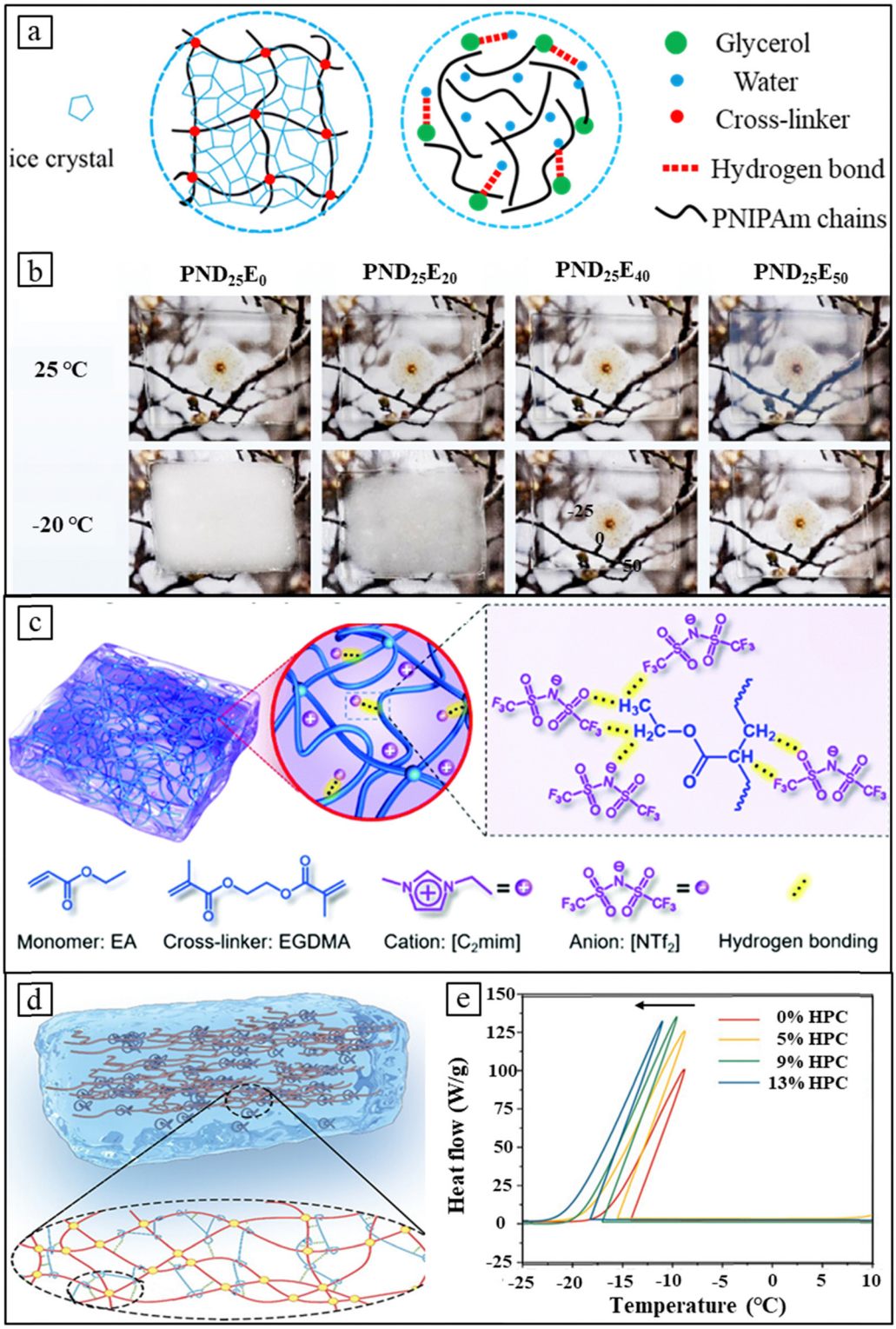



Fig. 6 Design strategies for anti-freezing thermochromic hydrogels. (a) A comparison between covalently crosslinked PNIPAm hydrogels and physically crosslinked counterparts reveals that the introduction of glycerol prevents physical crosslinked hydrogels from freezing below 0 °C. Reproduced with permission from ref. 88. Copyright 2023, The Royal Society of Chemistry. (b) Photographs of $PND_{25}E_0$, $PND_{25}E_{20}$, $PND_{25}E_{40}$ and $PND_{25}E_{50}$ hydrogels at 25 °C and −20 °C after 24 hours, where varying amounts of ethylene glycol (EG) and *N*-dimethylacrylamide (DMAA) are added, denoted as $PND_xE_y$. Reproduced with permission from ref. 96. Copyright 2023, Elsevier. (c) Incorporation of ionic liquids into thermochromic hydrogels enhances anti-freezing performance by forming hydrogen bonds between [$NTf_2$] and the matrix. Reproduced with permission from ref. 97. Copyright 2020, The Royal Society of Chemistry. (d) PNIPAm–HPC hydrogel fabricated by compositing with HPC shows significantly increased hydrogen bond density. (e) DSC curve for PNIPAm–HPC system hydrogels. (d) and (e) Reproduced with permission from ref. 48. Copyright 2023, Wiley-VCH.

Published on 18 September 2024. Downloaded by University of the Witwatersrand on 12/12/2024 3:02:43 PM.

as its integration with solar panels/perovskites or thermoelectric technology to generate power, thereby achieving higher energy-saving efficiency.

**3.3.1 Radiative cooling.** Radiative cooling materials emit long-wave infrared (LWIR) radiation into cold outer space, providing an effective cooling mechanism particularly suited for hot seasons and contributing to the development of energy-efficient smart windows.[99,100] This process efficiently lowers the surface temperature of objects without consuming energy by leveraging the atmospheric transparency window (8–13 μm) to dissipate excess heat into space. Integrating radiative cooling with thermochromic technology enhances the energy-saving capabilities of smart windows, particularly during hot summer periods. Radiative cooling can be classified into passive and switchable modes depending on whether its emissivity is adjustable.

*Passive radiative cooling.* Hydrogel-based thermochromic smart windows can achieve high infrared emissivity for passive radiative cooling through two main approaches. The first approach involves combing the thermochromic hydrogels with transparent radiative cooling film, such as polyethylene terephthalate (PET),[101] polyethylene (PE),[102–104] polyvinylidene fluoride (PVDF),[96,105] polymethyl methacrylate (PMMA)[106] or others,[107] to encapsulate the thermochromic hydrogel. As shown in Fig. 7a, Mei *et al.*[105] developed a sandwiched structure consisting of a thermochromic PNIPAm hydrogel enclosed within PVDF films. PVDF is known for its high infrared emissivity in the 8–13 μm wavelength range due to C–F molecular bonds. The resulting film exhibits significant modulation of visible light transmittance (86.3%) and achieves a high longwave infrared emissivity of 0.96 (Fig. 7b and c). Another approach involves integrating high-emissivity materials into the three-dimensional network structure of the thermochromic hydrogel. Guo *et al.*[91] developed a composite hydrogel composed of PNIPAm doped with $Na_2SiO_3$. The silicate ion in $Na_2SiO_3$ exhibits strong absorption at 10 μm wavelengths due to Si–O bond vibrations, resulting in a high atmospheric window emissivity of 0.962. As a result, the smart window demonstrates a substantial temperature reduction of 12.3 °C under direct sunlight.

*Switchable radiative cooling.* It's important to note that while many radiative cooling materials exhibit a fixed high emissivity in the long-wave infrared ($\varepsilon_{LWIR}$), crucial for radiative cooling at high temperatures, they also continue radiating heat outward, which is undesirable during low temperatures (winter). Therefore, there is a critical need to develop smart windows capable of dynamically adapting to varying solar radiation and weather conditions to optimize building energy efficiency.[108–110] An ideal radiative cooling thermochromic smart window should have the following characteristics (Fig. 7d): during cold seasons, it should maximize solar transmittance to capture external solar energy, while minimizing thermal emittance to retain internal heat. Conversely, in hot seasons, the window should reduce solar transmittance to block external solar heat gain, while maximizing thermal emittance to enhance internal heat dissipation. Several thermochromic-radiative cooling smart windows have been developed with adjustable emissivity in the infrared through structural design. Wang *et al.*[15] fabricated a revolutionary smart window with different emissivity (0.61 and 0.21) to regulate radiative cooling automatically (Fig. 7e), pioneering the development of self-adaptive radiative cooling thermochromic smart windows, while the $T_{lum}$ (~40%) and $\Delta T_{solar}$ (~10%) of the thermochromic smart window appears somewhat low.

To achieve high thermochromic performance and enable adaptive control of radiative cooling emissivity, Lin *et al.*[111] developed a solar and thermal regulatory (STR) window consisting of a PNIPAm hydrogel film grafting in the PDMS tray and a silver nanowire (AgNW) mesh on the hydrogel film. Due to the temperature-triggered hydration and dehydration of PNIPAm hydrogels, the thermochromic window exhibited remarkable solar modulation (cold: $T_{sol}$ = 65.5%, hot: $T_{sol}$ = 7.1%, $\Delta T_{sol}$ = 58.4%) and thermal modulation (cold: $R_{the}$ = 64.8%, hot: $R_{the}$ = 7.7%, $\Delta\varepsilon$ = 57.1%). This window effectively regulated indoor temperatures during both day and night, and in cold or hot environments, thereby achieving energy savings across all weather conditions.

By incorporating NIR/MIR regulating components (metal oxide low-E layer: ITO) and visible regulating/high-emission components (glass, PE layers, HPC hydrogel), thermochromic smart windows with controlled emissivity were successfully developed.[103] The resulting smart window exhibited a high $T_{lum}$ of 71.6% at room temperature and $\Delta T_{sol}$ of 50.3%. By flipping the window panel, it achieved a high front-side emissivity ($\varepsilon_{front}$) of 0.95 in summer and a low emissivity of 0.1 in winter, thereby meeting seasonal demands effectively. Similarly, a dual-control smart window for solar and radiative cooling was developed by integrating thermal-responsive hydrogels with an out-of-plane reconfigurable kirigami structure.[112,113] In summer, the high-emissivity PDMS kirigami covered the exterior surface to enhance radiative cooling, while the hydrogel composite turned translucent to reduce solar transmission above its $\tau_c$. In winter, the kirigami structure stretched and opened to expose the low-emissivity AgNWs layer, suppressing radiative cooling while the smart hydrogel became transparent for solar radiation. However, these strategies require manual intervention, such as flipping or stretching, and cannot achieve spontaneous switching of emissivity or reflectivity.

**3.3.2 Power generation.** Currently, smart windows primarily focus on regulating light transmission without effectively harnessing solar energy. Solar energy, being clean and abundant, holds promise for addressing the global energy crisis. Therefore, integrating energy-saving and energy-generating capabilities in smart windows represents an appealing research avenue. This integration not only produces green electricity but also enhances the efficiency of windows and buildings, enabling both heat management and energy collection within a single system.

*Solar cells.* The integration of solar cells with thermochromic materials has shown promise in recent studies. Lin *et al.*[114]

 This journal is © The Royal Society of Chemistry 2024

Published on 18 September 2024. Downloaded by University of the Witwatersrand on 12/12/2024 3:02:43 PM.

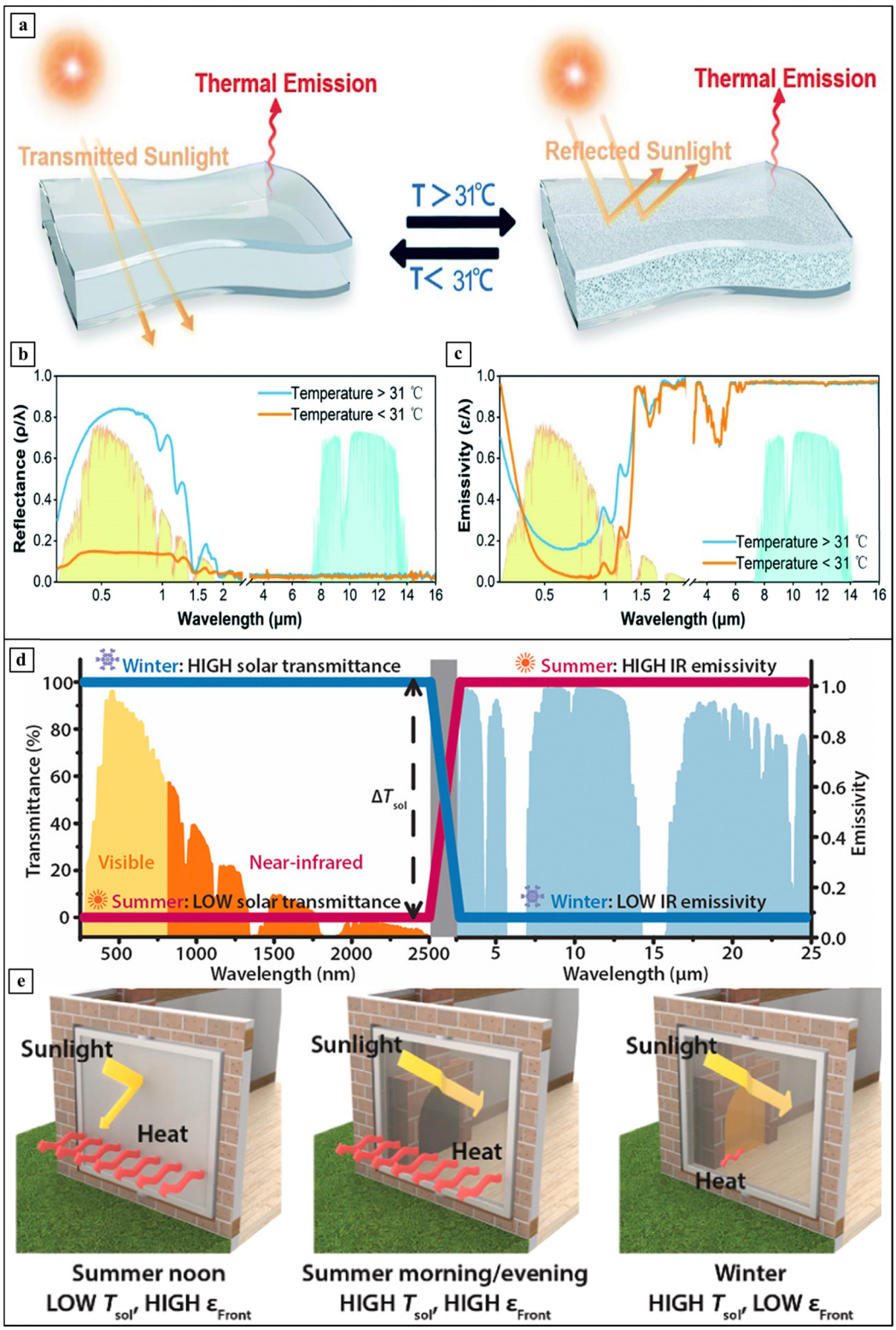



Fig. 7 Thermochromic hydrogel smart windows incorporating radiative cooling capabilities. (a) The schematic representation of the PVDF@PNIPAm film showcases PVDF films used as the top and bottom layers to encapsulate the PNIPAm hydrogel in the middle. (b) Reflectance spectra and (c) emissivity spectra of the PVDF@PNIPAm film at different temperatures. (a)–(c) Reproduced with permission from ref. 105. Copyright 2022, The Royal Society of Chemistry. (d) Transmittance spectra of the ideal thermochromic smart windows with adjustable emissivity. (e) The working principle of thermochromic smart windows in different seasons. (d) and (e) Reproduced with permission from ref. 103. Copyright 2021, Elsevier.

Published on 18 September 2024. Downloaded by University of the Witwatersrand on 12/12/2024 3:02:43 PM.

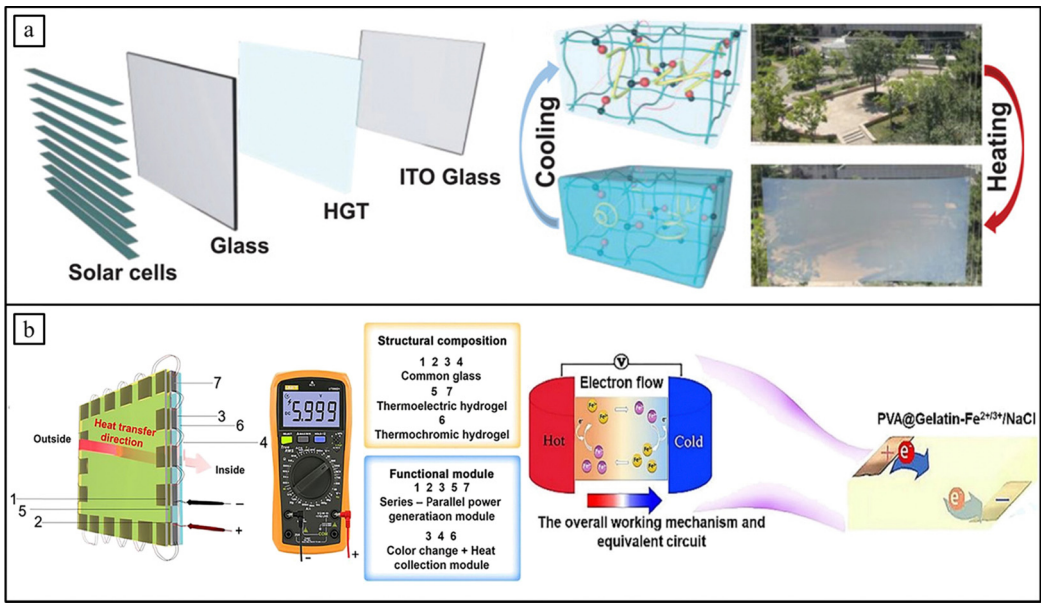



Fig. 8 Thermochromic hydrogel smart windows with power generation function. (a) Schematic illustration of the smart window integrated with solar cells. The right image depicts the mechanism of the thermochromic hydrogel along with optical photos. Reproduced with permission from ref. 115. Copyright 2022, Wiley-VCH. (b) Schematic diagram of a smart window containing both thermochromic and thermoelectric hydrogels. The right image shows the working mechanism of the PVA@gelatin-$Fe^{2+/3+}$/NaCl thermoelectric hydrogel. Reproduced with permission from ref. 118. Copyright 2024, Elsevier.

developed a thermotropic solar cell using halide perovskite cesium lead iodide/bromide, achieving a photoelectric conversion efficiency (PCE) of 7%. However, its phase transition temperature of 105 °C limits its application in smart window technology. Thermochromic hydrogels, featuring tunable phase transition temperatures, can be seamlessly integrated with solar cells, enabling both solar energy harvesting and temperature regulation functionalities. Niu *et al.*[115] introduced an innovative smart window design featuring a multi-layer louver structure that integrates a silicon solar cell, thermochromic HPC-PAM-PAA hydrogel (Fig. 8a), and ITO glass. This integration achieved a notable photoelectric conversion efficiency (PCE) of 18.24% along with excellent optical characteristics, including a $T_{lum}$ of approximately 90% and a $\Delta T_{sol}$ of 54%. Importantly, the solar cell can supply electricity to the ITO glass for actively adjusting the hydrogel's transmittance, while also providing anti-freezing capabilities. However, the inherent opacity of solar panels restricts visibility through the window to certain angles (between 90° and 60°). To address this limitation, Meng *et al.*[116,117] proposed several integrated photovoltaic smart windows with energy modulation and energy generation capabilities. This innovation combines semi-transparent perovskite with HPC hydrogel, achieving average visible transmittance of 27.3% (20 °C) and 10.4% at temperatures above 40 °C with a $\Delta T_{sol}$ of 15.7%.[117] Additionally, the smart window boasts a high PCE of 17.5%. The integration of semi-transparent perovskite solar cells ensures transparency from all angles below the $\tau_c$.

*Thermoelectric generators.* Due to temperature variations across the window, thermoelectric generators (TEGs) can harness this difference to generate power in conjunction with thermochromic smart windows. Xie *et al.*[118] demonstrated this concept by integrating a thermochromic PNIPAm hydrogel with a thermoelectric power generation PVA@gelatin-$Fe^{2+/3+}$/NaCl hydrogel (Fig. 8b). This integrated system not only regulates temperature but also converts temperature gradients between the window's interior and exterior into electrical energy. By embedding thermoelectric materials into the glass pane of the smart window, they achieved a continuous and stable current of approximately 75 μA with a 40 °C temperature difference. This electricity can help meet various energy needs within buildings, supporting functions such as lighting, ventilation, and other operational requirements.

The integration of solar cells, perovskites, and thermoelectric hydrogels into smart windows has enabled the merging of solar modulation and energy harvesting systems, effectively utilizing window components for power-generating capability, enhancing the overall energy-saving potential of these windows. However, significant challenges persist, such as low power generation efficiency, complex manufacturing processes, and high costs, all of which must be addressed to enable widespread adoption.

## 4 Summary and perspective

This review systematically reviews thermochromic smart windows based on thermo-responsive hydrogels, addressing fabrication strategies, chromic mechanisms, and recent advancements in responsiveness, stability, and energy-saving performance. Key developments, such as dual-responsiveness, broadened

 This journal is © The Royal Society of Chemistry 2024

Published on 18 September 2024. Downloaded by University of the Witwatersrand on 12/12/2024 3:02:43 PM.

$\tau_c$, freezing resistance, radiative cooling, and power generation, are highlighted. Additionally, we offer a perspective on future research directions in this field.

The fabrication of thermochromic hydrogels can be classified into three main types based on their chromic mechanisms. The first type includes hydrogels with inherent thermo-responsive properties, such as PNIPAm, which are typically synthesized *via* free radical polymerization and exhibit coil–globule transitions of polymer chains. The second type involves incorporating thermo-responsive SDS micelles into the highly transparent hydrogel matrixes, where the micelles undergo reversible aggregation and dissociation in response to temperature changes. The third category combines features from both the first and second types, such as PNIPAm/SDS hybrid hydrogels, which are commonly synthesized using a classical one-pot method. These hybrid hydrogels exhibit multiple response characteristics, undergoing an opaque–transparent–opaque transition as the temperature increases, thereby meeting the demands of various application scenarios.

We also highlight the advances in responsiveness, stability, and energy-saving performance of hydrogel-based thermochromic smart windows, which are crucial for practical application. Responsiveness includes two aspects. First, the development of dual-responsive smart windows. Thermo-electro dual-responsive smart windows offer active control with multiple switching modes, though this comes with increased power consumption. Thermo-photo dual-responsive windows enhance response speed by incorporating high-absorbance photothermal materials, though they experience a decrease in overall transmittance. Second, broadening the $\tau_c$ range through copolymerization or the addition of alcohols and salts adapts hydrogels for diverse climates and regions. Stability is enhanced by addressing the freezing issue, as the water in the hydrogel network is prone to freezing, which can damage the hydrogel structure. Stability improvements are achieved by adding alcohols, ionic liquids, and modifying the hydrogel networks. Energy-saving performance can be further optimized by integrating thermochromic technology with radiative cooling or power generation technology. Combining radiative cooling with thermochromic technology improves energy efficiency, particularly in hot climates, though it may increase heat loss in winter due to higher emissivity in the long-wave infrared spectrum. Switchable radiative cooling technology integrated with thermochromic hydrogels effectively addresses this issue. Furthermore, integrating silicon/perovskite solar cells or thermoelectric generators with thermochromic hydrogel enables simultaneous sunlight modulation and power generation, though challenges such as low power generation efficiency, complex manufacturing, and high costs must be considered.

There are still some challenges with thermochromic hydrogel-based smart windows. Firstly, the stability of thermochromic hydrogels needs to be further improved. While traditional building windows are designed to last for 10 years or more, current thermo-responsive hydrogels are typically evaluated for only 100 to 1000 cycles, which is insufficient for assessing their long-term durability. Furthermore, existing evaluation methods often partially consider the impact of temperature changes on the window's transmittance, neglecting practical weather factors, such as ultra-high temperatures (far beyond $\tau_c$), cold climates, intense ultraviolet exposure, and wet weather. Secondly, thermochromic hydrogels strongly rely on the sandwich structure (glass–hydrogel–glass). This design poses challenges for retrofitting existing windows and complicates the replacement and maintenance of thermo-responsive hydrogels. Recent advancements include electrochromic and photochromic films that can be directly applied to standard glass, offering a means to upgrade conventional windows. Therefore, transitioning away from the traditional sandwich structure to develop thermochromic hydrogel films for smart windows is crucial for their widespread application. Moreover,

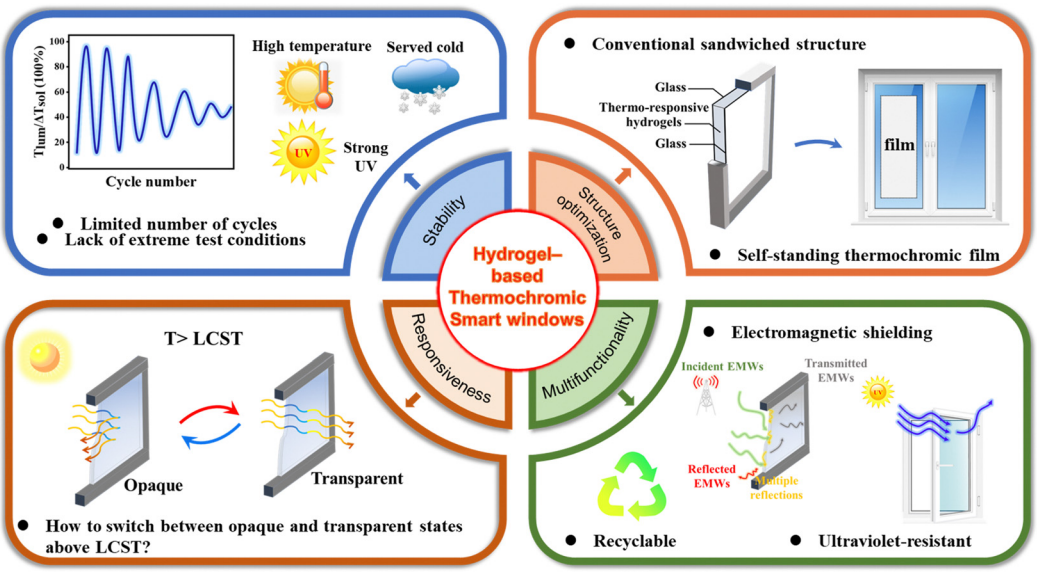



Fig. 9 Outlook of future thermochromic hydrogel-based smart windows.

Published on 18 September 2024. Downloaded by University of the Witwatersrand on 12/12/2024 3:02:43 PM.

improving the responsiveness of thermo-responsive hydrogels is essential, especially the transition between opaque and transparent states at high temperatures. Current thermochromic smart windows based on LCST behavior can regulate solar transmission and improve energy efficiency at the cost of visibility at higher temperature, thereby neglecting the need for adequate indoor lighting during summer or hot daytime conditions. The ideal thermochromic smart window should be transparent at low temperatures to allow solar radiation to enter, and opaque at high temperatures to block the entry of sunlight, but it can be switched from opaque state to transparent state at high temperatures according to personal preference. Finally, by optimizing the components or structural design, thermochromic hydrogels can be endowed with multifunctional properties such as UV protection, electromagnetic shielding, self-healing, sound insulation, and recyclability. These enhancements allow the hydrogels to meet the demands of various applications across multiple scenarios (Fig. 9).

Windows serve as a vital bridge between indoor environments and the outside world, significantly impacting the energy efficiency of buildings. The emerging thermochromic hydrogel represent a promising avenue for smart window technology, offering significant potential for enhancing energy efficiency in buildings. With increasing awareness of the importance of environmental protection and energy conservation, hydrogel-based thermochromic smart windows are set to unlock new opportunities. In the future, these windows are expected to evolve toward increased intelligence, enhanced stability, and improved energy efficiency, thereby making significant contributions to energy conservation and emission reduction of buildings.

## Author contributions

Gang Xu: writing – review & editing, writing – original draft, conceptualization. Yucan Lu: writing – review & editing, writing – original draft. Xinguantong Zhou: writing – original draft, visualization. Nosipho Moloto: writing – original draft, investigation. Jiacheng Liu: writing – original draft, visualization, investigation. Song-Zhu Kure-Chu: writing – original draft, conceptualization. Takehiko Hihara: writing – original draft, conceptualization. Wei Zhang: writing – review & editing, writing – original draft, funding acquisition, supervision, conceptualization, project administration. ZhengMing Sun: writing – review & editing, writing – original draft, funding acquisition, supervision.

## Data availability

Data availability is not applicable to this article as no new data were created or analyzed in this study.

## Conflicts of interest

The authors declare that they have no known competing financial interests or personal relationships that could have appeared to influence the work reported in this paper.

## Acknowledgements

This work is supported by the National Key Research and Development Program of China (No. 2023YFC3009502), the National Natural Science Foundation of China (No. 52371134, U23A20574), the Natural Science Foundation of Jiangsu Province (No. BK20231432), the Aeronautical Science Foundation of China (No. 2023Z015069001), and the Fundamental Research Funds for the Central Universities (No. 2242023K40027).

## References

1 Z. Zhang, L. Zhang, Y. Zhou, Y. Cui, Z. Chen, Y. Liu, J. Li, Y. Long and Y. Gao, *Chem. Rev.*, 2023, **123**, 7025.
2 M. González-Torres, L. Pérez-Lombard, J. F. Coronel, I. R. Maestre and D. Yan, *Energy Rep.*, 2022, **8**, 626.
3 International Energy Agency (2023), World Energy Outlook 2023, IEA, Paris **https://www.iea.org/reports/world-energy-outlook-2023**.
4 M. W. Akram, M. Hasannuzaman, E. Cuce and P. M. Cuce, *Energy Built Environ.*, 2023, **4**, 206.
5 Y. Zhou, X. Dong, Y. Mi, F. Fan, Q. Xu, H. Zhao, S. Wang and Y. Long, *J. Mater. Chem. A*, 2020, **8**, 10007.
6 S. Zhao, B. Wang, N. Zhu, Y. Huang, F. Wang, R. Li, Y. Zhao, Q. Jiang, X. Wu and R. Zhang, *Carbon Neutralization*, 2023, **2**, 4.
7 C. Gu, A.-B. Jia, Y.-M. Zhang and S. X.-A. Zhang, *Chem. Rev.*, 2022, **122**, 14679.
8 M. N. Mustafa, M. A. Mohd Abdah, A. Numan, A. Moreno-Rangel, A. Radwan and M. Khalid, *Renewable Sustainable Energy Rev.*, 2023, **181**, 113355.
9 W. Meng, A. J. J. Kragt, Y. Gao, E. Brembilla, X. Hu, J. S. van der Burgt, A. P. H. J. Schenning, T. Klein, G. Zhou, E. R. van den Ham, L. Tan, L. Li, J. Wang and L. Jiang, *Adv. Mater.*, 2024, **36**, 2304910.
10 S. Bhupathi, S. Wang, Y. Ke and Y. Long, *Mater. Sci. Eng., R*, 2023, **155**, 100747.
11 B. A. Rosales, J. Kim, V. M. Wheeler, L. E. Crowe, K. J. Prince, M. Mirzokarimov, T. Daligault, A. Duell, C. A. Wolden, L. T. Schelhas and L. M. Wheeler, *Adv. Energy Mater.*, 2023, **13**, 2203331.
12 Y. Ma, Y. Wang, J. Zhou, Y. Lan, S. Jiang, Y. Ge, S. Tan, S. Zhang, C. Wang and Y. Wu, *Mater. Horiz.*, 2024, **11**, 3825.
13 Y. Deng, Y. Yang, Y. Xiao, X. Zeng, H. L. Xie, R. Lan, L. Zhang and H. Yang, *Adv. Mater.*, 2024, **36**, 2401869.
14 Y. Xue and S. Yin, *Nanoscale*, 2022, **14**, 11054.
15 S. Wang, T. Jiang, Y. Meng, R. Yang, G. Tan and Y. Long, *Science*, 2021, **374**, 1501.
16 Z. Shao, A. Huang, C. Cao, X. Ji, W. Hu, H. Luo, J. Bell, P. Jin, R. Yang and X. Cao, *Nat. Sustainable*, 2024, **7**, 796.
17 S. Liu, Y. W. Du, C. Y. Tso, H. H. Lee, R. Cheng, S. Feng and K. M. Yu, *Adv. Funct. Mater.*, 2021, **31**, 2010426.
18 S. Liu, Y. Du, R. Zhang, H. He, A. Pan, T. C. Ho, Y. Zhu, Y. Li, H. Yip, A. K. Y. Jen and C. Y. Tso, *Adv. Mater.*, 2024, **36**, 2306423.

 This journal is © The Royal Society of Chemistry 2024

Published on 18 September 2024. Downloaded by University of the Witwatersrand on 12/12/2024 3:02:43 PM.

19 S. Liu, Y. Li, Y. Wang, Y. Du, K. M. Yu, H.-L. Yip, A. K. Y. Jen, B. Huang and C. Y. Tso, *Nat. Commun.*, 2024, **15**, 876.
20 B. Li, F. Xu, T. Guan, Y. Li and J. Sun, *Adv. Mater.*, 2023, **35**, 2211456.
21 C. Hong, B. Li, J. Zhang, Y. Li and J. Sun, *Adv. Funct. Mater.*, 2024, **34**, 2313781.
22 S. K. Saju, A. B. Puthirath, S. Wang, T. Tsafack, L. K. Beagle, A. Baydin, N. Chakingal, N. Komatsu, F. Tay, A. Sharma, R. Sreenivasan, J. Kono, R. Vajtai, N. R. Glavin, Y. Long and P. M. Ajayan, *Joule*, 2024, **8**, 1.
23 W. Zhang, R. Wang, Z. Sun, X. Zhu, Q. Zhao, T. Zhang, A. Cholewinski, F. Yang, B. Zhao, R. Pinnaratip, P. K. Forooshani and B. P. Lee, *Chem. Soc. Rev.*, 2020, **49**, 433.
24 H. Xia, G. Xu, X. Cao, C. Miao, H. Zhang, P. Chen, Y. Zhou, W. Zhang and Z. Sun, *Adv. Mater.*, 2023, **35**, 2301996.
25 P. Chen, Q. Ruan, R. Nasseri, H. Zhang, X. Xi, H. Xia, G. Xu, Q. Xie, C. Yi, Z. Sun, H. Shahsavan and W. Zhang, *Adv. Sci.*, 2022, **9**, 2204730.
26 Y. Zhou, S. Wang, J. Peng, Y. Tan, C. Li, F. Y. C. Boey and Y. Long, *Joule*, 2020, **4**, 2458.
27 Y. Zhou, Y. Cai, X. Hu and Y. Long, *J. Mater. Chem. A*, 2014, **2**, 13550.
28 Y.-S. Yang, Y. Zhou, F. B. Yin Chiang and Y. Long, *RSC Adv.*, 2016, **6**, 61449.
29 X. Cao, T. Chang, Z. Shao, F. Xu, H. Luo and P. Jin, *Matter*, 2020, **2**, 862.
30 M. K. Shahzad, R. Z. A. Manj, G. Abbas, R. A. Laghari, S. S. Akhtar, M. A. Khan, M. B. Tahir, S. Znaidia and M. Alzaid, *RSC Adv.*, 2022, **12**, 30985.
31 E. Koudoumas, K. T. Le and D. Vernardou, *Energy Nexus*, 2023, **11**, 100237.
32 Y. Liu, W. Lv, J. Feng, J. Tian, P. Wang, L. Xu, Y. Long and L. Yao, *Adv. Funct. Mater.*, 2024, 2402234, Early View.
33 A. Kanwat, N. Yantara, P. Kajal and N. Mathews, *Adv. Opt. Mater.*, 2024, **12**, 2301342.
34 R. Zhang, Z. Zhang, J. Han, L. Yang, J. Li, Z. Song, T. Wang and J. Zhu, *Light: Sci. Appl.*, 2023, **12**, 11.
35 G. Chen, Y. Zhang, Y. Chen and J. Fu, *J. Polym. Sci.*, 2023, **62**, 229.
36 S. Wu, H. Sun, M. Duan, H. Mao, Y. Wu, H. Zhao and B. Lin, *Cell Rep. Phys. Sci.*, 2023, **4**, 101370.
37 D. Wang, G. Chen and J. Fu, *J. Mater. Chem. A*, 2024, **12**, 12960.
38 S. Zhong, Y. Xue, K. Wang, L. Wang and T. Jiang, *Mater. Today Commun.*, 2024, **40**, 109506.
39 N. M. Mohammad, Y. Zhang, W. Xu, S. S. Aranke, D. Carne, P. Deng, F. Du, X. Ruan and T. Li, *Small*, 2024, **20**, 2303706.
40 R. L. Sala, R. H. Gonçalves, E. R. Camargo and E. R. Leite, *Sol. Energy Mater. Sol. Cells*, 2018, **186**, 266.
41 A. Urain, D. Minudri, D. Mantione, I. Calvo, N. Casado and D. Mecerreyes, *Sol. Energy Mater. Sol. Cells*, 2023, **259**, 112431.
42 F. Chen, X. Wu, G. Lu, J. Nie and X. Zhu, *ACS Appl. Mater. Interfaces*, 2024, **16**, 21013.
43 Z. Lin, Z. Yang and L. Gao, *Mater. Horiz.*, 2024, **11**, 3127.
44 K. Li, S. Meng, S. Xia, X. Ren and G. Gao, *ACS Appl. Mater. Interfaces*, 2020, **12**, 42193.
45 Y. Liu, Y. Guo, Z. Zhang, Z. Huang, P. Qi, J. Cui, A. Song and J. Hao, *Chem. Commun.*, 2020, **56**, 5315.
46 Z. Yu, Y. Yang, C. Shen, L. Mao, C. Cui, Z. Chen and Y. Zhang, *J. Mater. Chem. C*, 2023, **11**, 583.
47 Y. Gao, K. Li, X. Ren and G. Gao, *Chem. – Eur. J.*, 2023, **30**, 2302147.
48 Y. Feng, S. Wang, Y. Li, W. Ma, G. Zhang, M. Yang, H. Li, Y. Yang and Y. Long, *Adv. Funct. Mater.*, 2023, **33**, 2211027.
49 L. Xie, X. Wang, X. Zou, Z. Bai, S. Liang, C. Wei, S. Zha, M. Zheng, Y. Zhou, O. Yue and X. Liu, *Small*, 2023, **19**, 2304321.
50 K. Wang, G. Chen, S. Weng, L. Hou, D. Ye and X. Jiang, *ACS Appl. Mater. Interfaces*, 2023, **15**, 4385.
51 L. Zhang, H. Xia, F. Xia, Y. Du, Y. Wu and Y. Gao, *ACS Appl. Energy Mater.*, 2021, **4**, 9783.
52 M. Dai, J. Zhao, Y. Zhang, H. Li, L. Zhang, Y. Liu, Z. Ye and S. Zhu, *ACS Appl. Mater. Interfaces*, 2022, **14**, 53314.
53 Z. Yu, Y. Ma, L. Mao, Y. Lian, Y. Xiao, Z. Chen and Y. Zhang, *Mater. Horiz.*, 2024, **11**, 207.
54 T.-G. La, X. Li, A. Kumar, Y. Fu, S. Yang and H.-J. Chung, *ACS Appl. Mater. Interfaces*, 2017, **9**, 33100.
55 Y. Wang, X. Fang, S. Li, N. An, H. Pan and J. Sun, *SmartMat*, 2024, **5**, e1256.
56 J. Chen, G. Li, T. Jiang, S. Wang, H. Hu, Z. Bai, D. Shi, M. Chen, J. Guan, G. Tan and Y. Long, *Nano Energy*, 2024, **123**, 109386.
57 X.-H. Li, C. Liu, S.-P. Feng and N. X. Fang, *Joule*, 2019, **3**, 290.
58 J. Li, P. Gu, H. Pan, Z. Qiao, J. Wang, Y. Cao, W. Wang and Y. Yang, *Adv. Sci.*, 2023, **10**, 2206044.
59 G. Zhu, G. Xu, Y. Zhang, G. Lu, X. Cai, W. Zhang, S. Wei and C. Miao, *Research*, 2024, **7**, 0462.
60 L. Tang, L. Wang, X. Yang, Y. Feng, Y. Li and W. Feng, *Prog. Mater. Sci.*, 2021, **115**, 100702.
61 G. Chen, K. Wang, J. Yang, J. Huang, Z. Chen, J. Zheng, J. Wang, H. Yang, S. Li, Y. Miao, W. Wang, N. Zhu, X. Jiang, Y. Chen and J. Fu, *Adv. Mater.*, 2023, **35**, 2211716.
62 H. Peng, X. Yang, Y. Gu, Q. Yang, T. Lan, S. Chen and B. Yan, *J. Mater. Chem. A*, 2023, **11**, 17848.
63 G. Xu, H. Xia, P. Chen, W. She, H. Zhang, J. Ma, Q. Ruan, W. Zhang and Z. Sun, *Adv. Funct. Mater.*, 2022, **32**, 2109597.
64 X.-Z. Zhang, X.-D. Xu, S.-X. Cheng and R.-X. Zhuo, *Soft Matter*, 2008, **4**, 385.
65 Y. Nan, C. Zhao, G. Beaudoin and X. X. Zhu, *Macromol. Rapid Commun.*, 2023, **44**, 2300261.
66 Y. Liu, Y. Han, Z. Huang, P. Qi, A. Song and J. Hao, *Chem. Commun.*, 2022, **58**, 2814.
67 Y. Liu, C. Yan, P. Qi, A. Song and J. Hao, *Adv. Mater. Interfaces*, 2023, **10**, 2201885.
68 Y. Ke, J. Chen, G. Lin, S. Wang, Y. Zhou, J. Yin, P. S. Lee and Y. Long, *Adv. Energy Mater.*, 2019, **9**, 1902066.
69 L. Zhang, Y. Du, F. Xia and Y. Gao, *Chem. Eng. J.*, 2023, **455**, 140849.
70 S. Wang, Z. Xu, T. Wang, T. Xiao, X.-Y. Hu, Y.-Z. Shen and L. Wang, *Nat. Commun.*, 2018, **9**, 1737.

Published on 18 September 2024. Downloaded by University of the Witwatersrand on 12/12/2024 3:02:43 PM.

71 D. Ma, L. Chen, F. Fan, Q. Wang, G. Duan, L. Bi, L. Mei, K. Bi, Y. Chen and H. Duan, *ACS Appl. Mater. Interfaces*, 2022, **14**, 56065.
72 Y. Zhong, Y. Wang, Y. Zhou, Q. He, S. Ge, X. Liu, R. Xu and S. Feng, *ChemistrySelect*, 2021, **6**, 5496.
73 B. Deng, Y. Zhu, X. Wang, J. Zhu, M. Liu, M. Liu, Y. He, C. Zhu, C. Zhang and H. Meng, *Adv. Mater.*, 2023, **35**, 2302685.
74 M. Wang, X. Xing, I. F. Perepichka, Y. Shi, D. Zhou, P. Wu and H. Meng, *Adv. Energy Mater.*, 2019, **9**, 1900433.
75 Z. Xu, S. Wang, X. Y. Hu, J. Jiang, X. Sun and L. Wang, *Sol. RRL*, 2018, **2**, 1800204.
76 Q. Lei, L. Wang, H. Xie and W. Yu, *Build. Environ.*, 2022, **222**, 109407.
77 L. Zhang, Y. Du, H. Xia, F. xia, G. Yang and Y. Gao, *Ceram. Int.*, 2022, **48**, 37122.
78 Z. Yang, M. Zhang, X. Zhao, R. Hu, H. Zhao, S. Zeb, W. Jiang, T. Liu and X. Jiang, *Ceram. Int.*, 2024, **50**, 19543.
79 Y. Li, Y. Wang, J. Lu, W. Wang and D. Wang, *Chem. Eng. J.*, 2023, **457**, 141299.
80 M. Guo, Q. Yu, X. Wang, W. Xu, Y. Wei, Y. Ma, J. Yu and B. Ding, *ACS Appl. Mater. Interfaces*, 2021, **13**, 5634.
81 J. Tian, J. Gu, H. Peng, H. Wang, Z. Du, X. Cheng and X. Du, *Composites, Part A*, 2021, **149**, 106538.
82 J. Liu, H. Lu, Q. Huang, Z. Ding, R. Yang, M. Geng, M. Meng, Z. Liu and Y. Liu, *Sol. Energy Mater. Sol. Cells*, 2023, **263**, 112596.
83 Q. Lei, W. Yu, G. Xie, Y. Li, C. Wu, G. Jiang, Y. Zhou and H. Xie, *Sol. RRL*, 2023, **7**, 2200590.
84 C. Lu, L. Yang, B. Yan, L. Sun, P. Zhang, W. Zhang and Z. Sun, *Adv. Funct. Mater.*, 2020, **30**, 2000852.
85 J. Tao, S. Tian, B. Li, T. Ma, L. Zhou and X. Zhao, *Chem. Eng. J.*, 2024, **482**, 149079.
86 J. Tian, C. Jin, X. Wu, C. Liao, J. Xie and Y. Luo, *RSC Adv.*, 2023, **13**, 8923.
87 Q. Jiang, M. Chen, Z. Qin, Y. Li, J. Li and H. Zhang, *Chem. Eng. J.*, 2024, **489**, 151259.
88 G. Li, J. Chen, Z. Yan, S. Wang, Y. Ke, W. Luo, H. Ma, J. Guan and Y. Long, *Mater. Horiz.*, 2023, **10**, 2004.
89 Y. Ding, Y. Duan, F. Yang, Y. Xiong and S. Guo, *Chem. Eng. J.*, 2023, **460**, 141572.
90 H. Du, R. Wickramasinghe and X. Qian, *J. Phys. Chem. B*, 2010, **114**, 16594.
91 R. Guo, Y. Shen, Y. Chen, C. Cheng, C. Ye and S. Tang, *Chem. Eng. J.*, 2024, **486**, 150194.
92 S. Xu, S. Wu, R. Zhu, Z. Qiu and Y. Yan, *Adv. Funct. Mater.*, 2024, DOI: **10.1002/adfm.202405965**.
93 Y. Jian, S. Handschuh-Wang, J. Zhang, W. Lu, X. Zhou and T. Chen, *Mater. Horiz.*, 2021, **8**, 351.
94 H. Zhang, K. Xue, C. Shao, S. Hao and J. Yang, *Chem. Mater.*, 2023, **35**, 10316.
95 X. Huang, Z. Zheng, H. Wang, W. Xu, M. Wu, M. Wang, C. Chen, L. Wan, R. Du, T. Zhu, Z. Huang, X. Wang, X. Wang, Q. Zhang and X. Jia, *Adv. Funct. Mater.*, 2024, **34**, 2312149.
96 K. Wang, L. Zhang and X. Jiang, *J. Colloid Interface Sci.*, 2023, **652**, 663.
97 Z. Cao, H. Liu and L. Jiang, *Mater. Horiz.*, 2020, **7**, 912.
98 Y. Mao, L. Wang, Z. Wu, D. Ji, H. Sheng, X. Chang and Y. Zhu, *Compos. Commun.*, 2023, **44**, 101769.
99 Y. H. Chan, Y. Zhang, T. Tennakoon, S. C. Fu, K. C. Chan, C. Y. Tso, K. M. Yu, M. P. Wan, B. L. Huang, S. Yao, H. H. Qiu and C. Y. H. Chao, *Energy Convers. Manage.*, 2022, **272**, 116342.
100 R. Liu, S. Wang, Z. Zhou, K. Zhang, G. Wang, C. Chen and Y. Long, *Adv. Mater.*, 2024, 2401577, DOI: **10.1002/adma.202401577**.
101 N. Guo, S. Liu, C. Chen, C. Song, S. Mo, H. Yan and M. Chen, *Sol. Energy*, 2024, **270**, 112405.
102 Y. Wang, X. Tan, X. Yang, G. Qi and Y. Tu, *Sol. Energy Mater. Sol. Cells*, 2024, **271**, 112871.
103 S. Wang, Y. Zhou, T. Jiang, R. Yang, G. Tan and Y. Long, *Nano Energy*, 2021, **89**, 106440.
104 J. Chen, G. Li, T. Jiang, S. Wang, H. Hu, Z. Bai, D. Shi, M. Chen, J. Guan, G. Tan and Y. Long, *Nano Energy*, 2024, **123**, 109386.
105 X. Mei, T. Wang, M. Chen and L. Wu, *J. Mater. Chem. A*, 2022, **10**, 11092.
106 R. Zhang, R. Li, P. Xu, W. Zhong, Y. Zhang, Z. Luo and B. Xiang, *Chem. Eng. J.*, 2023, **471**, 144527.
107 L. Hu, C. Wang, H. Zhu, Y. Zhou, H. Li, L. Liu and L. Ma, *Small*, 2024, **20**, 2306823.
108 H. Tang, C. Guo, F. Fan, H. Pan, Q. Xu and D. Zhao, *Energy Environ. Sci.*, 2024, **17**, 4498.
109 Z. Wang, S.-K. Kim and R. Hu, *Matter*, 2022, **5**, 780.
110 K. Tang, K. Dong, J. Li, M. P. Gordon, F. G. Reichertz, H. Kim, Y. Rho, Q. Wang, C.-Y. Lin, C. P. Grigoropoulos, A. Javey, J. J. Urban, J. Yao, R. Levinson and J. Wu, *Science*, 2021, **374**, 1504.
111 C. Lin, J. Hur, C. Y. H. Chao, G. Liu, S. Yao, W. Li and B. Huang, *Sci. Adv.*, 2022, **8**, eabn7359.
112 H. Yin, X. Zhou, Z. Zhou, R. Liu, X. Mo, Z. Chen, E. Yang, Z. Huang, H. Li, H. Wu, J. Zhou, Y. Long and B. Hu, *Research*, 2023, **6**, 0103.
113 S. Wang, Y. Dong, Y. Li, K. Ryu, Z. Dong, J. Chen, Z. Dai, Y. Ke, J. Yin and Y. Long, *Mater. Horiz.*, 2023, **10**, 4243.
114 J. Lin, M. Lai, L. Dou, C. S. Kley, H. Chen, F. Peng, J. Sun, D. Lu, S. A. Hawks, C. Xie, F. Cui, A. P. Alivisatos, D. T. Limmer and P. Yang, *Nat. Mater.*, 2018, **17**, 261.
115 Y. Niu, Y. Zhou, D. Du, X. Ouyang, Z. Yang, W. Lan, F. Fan, S. Zhao, Y. Liu, S. Chen, J. Li and Q. Xu, *Adv. Sci.*, 2022, **9**, 2105184.
116 Y. Meng, X. Li, S. Wang, C. Lau, H. Hu, Y. Ke, G. Tan, J. Yang and Y. Long, *Nano Energy*, 2022, **91**, 106632.
117 Y. Meng, Y. Tan, X. Li, Y. Cai, J. Peng and Y. Long, *Appl. Energy*, 2022, **324**, 119676.
118 G. Xie, Y. Li, C. Wu, M. Cao, H. Chen, Y. Xiong, Y. Xu, H. Xie and W. Yu, *Chem. Eng. J.*, 2024, **481**, 148531.

 This journal is © The Royal Society of Chemistry 2024